

ANALYZING EARTHQUAKE CASUALTY RISK AT CENSUS BLOCK LEVEL:
A CASE STUDY IN THE LEXINGTON CENTRAL BUSINESS DISTRICT,
KENTUCKY

by

Jarod Thomas Hustler

A Thesis Presented to the
FACULTY OF THE USC GRADUATE SCHOOL
UNIVERSITY OF SOUTHERN CALIFORNIA
In Partial Fulfillment of the
Requirements for the Degree
MASTER OF SCIENCE
(GEOGRAPHIC INFORMATION SCIENCE AND TECHNOLOGY)

August 2014

DEDICATION

This work is dedicated to all of the hard working individuals who put themselves in harm's way to help others in distress. This includes, but is not limited to, the first responders, disaster relief volunteers and all of those who help support them in difficult times. God Bless you and it is my hope that this study can improve upon your future heroic efforts.

ACKNOWLEDGMENTS

I would like to thank my thesis chair, Dr. Flora Paganelli, for her assistance in this long process. I really appreciate all of the support and guidance she has provided to complete this project. I would also like to thank my thesis committee members, Dr. Su Jin and Dr. Yao-Yi Chiang, and everyone within the SSI department at USC that has helped me throughout the entire Master's program. Thank you to Dr. Junfeng Zhu of the Kentucky Geological Survey for providing the LiDAR data created by Photo Science, Inc.

Table of Contents

DEDICATION.....	ii
ACKNOWLEDGMENTS	iii
LIST OF TABLES	vi
LIST OF FIGURES	vii
LIST OF ABBREVIATIONS	viii
ABSTRACT.....	ix
CHAPTER 1: INTRODUCTION AND LITERATURE REVIEW.....	1
1.1 Introduction	1
1.2.1 <i>Earthquake Studies Using Remote Sensing – Light Detection and Ranging (LiDAR)..</i>	<i>5</i>
1.2.2 <i>Earthquake Studies Using GIS: HAZUS Application.....</i>	<i>7</i>
1.2.3 <i>Population Estimation Studies</i>	<i>9</i>
CHAPTER 2: STUDY AREA AND SEISMIC HISTORY OF AREA	12
2.1 Study Area.....	12
2.2 Seismic History of the Study Area	13
2.2.1 <i>New Madrid Seismic Zone (NMSZ).....</i>	<i>13</i>
2.2.2 <i>Wabash Valley Seismic Zone.....</i>	<i>14</i>
2.2.3 <i>Earthquakes and Faults Near the Study Area</i>	<i>15</i>
CHAPTER 3: DATA SOURCES AND METHODOLOGY.....	17
3.1 Data Sources.....	18
3.1.1 <i>Census Data</i>	<i>18</i>
3.1.2 <i>LiDAR Data.....</i>	<i>19</i>
3.1.3 <i>Parcel and Ancillary Data</i>	<i>20</i>
3.2 Pre-processing Data.....	21
3.2.1 <i>Census Pre-processing: Estimating Daytime Populations By Parcel.....</i>	<i>21</i>
3.2.2 <i>Pre-processing LiDAR Data</i>	<i>23</i>
3.2.3 <i>Pre-processing Parcel Data.....</i>	<i>24</i>
3.2.4 <i>Changes to Pre-processing Based on Study Area Data Acquisition.....</i>	<i>25</i>
3.3 Methodology.....	27
3.3.1 <i>HAZUS-MH Methodology.....</i>	<i>28</i>
3.3.2 <i>UDSCE Method at Census Tract Level.....</i>	<i>30</i>
3.3.3 <i>UDSCE Method at Census Block Level</i>	<i>36</i>
CHAPTER 4: RESULTS	38
4.1 HAZUS-MH Results.....	39
4.2 UDSCE Method at Census Tract Level Results.....	42
4.2.1 <i>Validation of UDSCE Method.....</i>	<i>43</i>
4.3 UDSCE Method at Census Block Level Results	45
4.4 UDSCE Method at Parcel Level Results	47
CHAPTER 5: CONCLUSIONS AND FUTURE WORK.....	49
5.1 Conclusions	49
5.2 Future Work	50
5.2.1 <i>Data Availability</i>	<i>51</i>
5.2.2 <i>Flexibility of UDSCE Method</i>	<i>51</i>

5.2.3 <i>Study Area Constraints</i>	52
5.2.4 <i>Population Estimations</i>	52
5.2.5 <i>Time Factors Affecting Estimates</i>	53
REFERENCES	54
APPENDIX A: Indoor Casualty Rates by Model Building Type for Slight Structural Damage	58
APPENDIX B: Indoor Casualty Rates by Model Building Type for Moderate Structural Damage	59
APPENDIX C: Indoor Casualty Rates by Model Building Type for Extensive Structural Damage	60
APPENDIX D: Indoor Casualty Rates by Model Building Type for Complete Structural Damage (No Collapse)	61
APPENDIX E: Indoor Casualty Rates by Model Building Type for Complete Structural Damage (With Collapse)	62
APPENDIX F: Explanation of Building Types	63

LIST OF TABLES

Table 1:	Census Data Specifications	19
Table 2:	LiDAR Data Characteristics	19
Table 3:	Parcel and Other ArcGIS Data Specifications	20
Table 4:	Breakdown of Office Worker Population by Census Tract	23
Table 5:	Alternate Formats of Datasets Used For UDSCE Method	26
Table 6:	Description of Injury Severity Levels for HAZUS-MH	28
Table 7:	HAZUS-MH Default Setting For Population Distribution	29
Table 8:	Building Material Scores	32
Table 9:	Building Height Scores	33
Table 10:	Building Age Scores	34
Table 11:	Total Score Ratings	34
Table 12:	UDSCE Casualty Rates by Damage State	35
Table 13:	Examples of Vulnerability Calculation by Parcel	36
Table 14:	Examples of Casualty Calculation by Parcel	36
Table 15:	HAZUS-MH Casualty Estimates for 5.5 Magnitude Earthquake	40
Table 16:	HAZUS-MH Casualty Estimates for 6.2 Magnitude Earthquake	41
Table 17:	HAZUS-MH Casualty Estimates for 6.8 Magnitude Earthquake	41
Table 18:	UDSCE Method For Study Area Results	43
Table 19:	Comparison of HAZUS-MH and UDSCE Results	44
Table 20:	Percent Difference Error Analysis of Results	45

LIST OF FIGURES

Figure 1:	LiDAR Image of Urban Area	6
Figure 2:	Study Area Map	12
Figure 3:	Map of Fault Lines in Central Kentucky	16
Figure 4:	Workflow of Earthquake Casualty Estimation	17
Figure 5:	Map of Office Square Footage for Census Tract	22
Figure 6:	Raw LiDAR Points of Study Area	24
Figure 7:	LiDAR Preprocessing Flowchart	25
Figure 8:	Parcel Preprocessing Flowchart	26
Figure 9:	Map of Study Area Parcels	27
Figure 10:	HAZUS-MH Earthquake Methodology Flowchart	29
Figure 11:	UDSCE Method Flowchart	31
Figure 12:	Modelbuilder Design of UDSCE Method by Census Tract	37
Figure 13:	Modelbuilder Design of UDSCE Method by Census Block	37
Figure 14:	Map of Earthquake Epicenter	38
Figure 15:	HAZUS-MH Total Casualty Maps by Magnitude	40
Figure 16:	UDSCE Method Total Casualties in Study Area Map	42
Figure 17:	Estimation of Casualties by Census Block	46
Figure 18:	Census Block Casualties by Land Use	46
Figure 19:	Estimation of Casualties by Parcel	48

LIST OF ABBREVIATIONS

CBD	Central Business District
CUSEC	Central United States Earthquake Consortium
FEMA	Federal Emergency Management Agency
GIS	Geographic Information Systems
HAZUS-MH	Hazards United States Multi-Hazard
KGS	Kentucky Geological Survey
KRFS	Kentucky River Fault System
LFUCG	Lexington-Fayette Urban County Government
LiDAR	Light Detection and Ranging
NEHRP	National Earthquake Hazards Reduction Program
NMSZ	New Madrid Seismic Zone
PDE	Percentage Difference Error
PVA	Property Valuation Administrator
UDSCE	Urban Daytime Seismic Casualty Estimation
USGS	United States Geological Survey
WVSZ	Wabash Valley Seismic Zone

ABSTRACT

Earthquakes strike without warning and leave a trail of devastation. To better prepare for these disastrous events, government agencies must have a comprehensive emergency management plan based on current spatial and non-spatial data. Applications such as HAZUS-MH, developed by the Federal Emergency Management Agency (FEMA), can be used with ArcGIS software to model loss estimations for many natural disaster scenarios. However, HAZUS-MH does not supply the necessary data to analyze losses at geographic units smaller than the census tract level, limiting its effectiveness for an urban area earthquake casualty study.

Focusing on the Central Business District (CBD) of Lexington (Kentucky), this study developed a new methodology to test alternate input such as locally sourced LiDAR remote sensing data and Geographic Information System (GIS) -based parcels data to predict earthquake casualties within an urban area. The Urban Daytime Seismic Casualty Estimation (UDSCE) method was applied at a census tract level and casualty estimations validated using the HAZUS-MH model results from three simulated earthquake scenarios. The UDSCE methodology was then applied at the census block and parcel level to refine estimates counts at higher resolution.

The results show compelling evidence that working at the census block and parcel level can provide focalized casualty counts within the urban context, thus providing emergency planners crucial information to better prepare for earthquake events in commercial/urban densely populated areas.

CHAPTER 1: INTRODUCTION AND LITERATURE REVIEW

Chapter 1 provides an introduction on my personal interest in earthquake hazard events and the importance of earthquake hazard modeling and damage estimates made possible with advanced technologies such as GIS. This is followed by a literature review in relation to earthquake hazard events and damage estimates using Remote Sensing and GIS is provided. The chapter ends with summary of the key the research questions and objectives of this thesis.

1.1 Introduction

I will never forget the first time I felt an earthquake. I was a fifth grader living in Southern California when a strong tremor hit the city of Whittier on the morning of 1 October, 1987. As I was getting dressed for school in my bedroom, everything around me started shaking. Initially I was frozen in place; after a few seconds my instincts kicked in and I climbed under my desk for safety. The many practice drills that my school conducted in preparation for an earthquake were finally put to the test. Fortunately, I lived far enough away from the epicenter to not experience any damage to my house and I was able to go to school. There were lots of interesting conversations that day with my classmates about what they experienced during the event. Some even wrote out their last wills!

A couple years after that experience I moved across the country, where earthquakes are virtually non-existent. I felt I would never have to worry again about being ready for an earthquake. I was wrong. A scientist predicted that a large earthquake would strike along the New Madrid Seismic Zone (NMSZ) in Missouri, potentially

affecting the community that I now called home (Show Me Net 2014). Many area school districts shut down that day, and even though my school was open, a large percentage of children stayed home. The predicted earthquake never happened and life went on as normal after that day.

These two events in my life, though completely opposite in nature, were stark reminders of the importance of being ready for disaster to happen at any time. In the first case, I had no warning of the impending seismic event. The benefit was that careful pre-planning allowed me to make an informed decision to protect myself the best I possibly could at that very moment. The second event (or lack thereof) frightened many people who were not sure what to do if the earthquake took place. Many questions were raised in my mind regarding the second event that I still think about to this day. What would have happened if there *was* an earthquake that day? Would the kids that stayed home that day have had a better chance of surviving than the ones that went to school? Did state and local emergency managers have the resources necessary at that time to deal with this kind of disaster to limit casualties? If so, were they flexible enough to make any changes to their execution of the plan if the disaster took place at a different time of day? These questions are difficult at best to answer unless the event actually took place, putting the emergency workers to the test.

As time has passed, technological advances have given researchers better perspective to answer these questions. Geographic information systems (GIS) software became a leader in combining data and methodologies to assess disaster risk such as casualties stemming from an earthquake (Esri 2008). The majority of injuries and deaths attributed to earthquakes are due to the damage of buildings and structures where people

are located at the time of the event (USGS 2014). In that regard, having accurate information of building structures and headcounts within those structures to add into a GIS database can lead to better prediction of casualties and their spatial distribution within the area of study.

Despite the rapid advancement of the capabilities to look at risk from seismic activity, there are several issues within the scientific community that impede the progress of the effectiveness of incorporating GIS in earthquake studies. For one, GIS and remote sensing technology show little, if any, improvement in predicting when and where an earthquake will take place (Gillespie et al. 2007). This limitation still leaves the study of estimating damages as purely hypothetical and many earthquake scenarios would have to be viewed for a particular study area, adding cost and time to such projects. Models could be validated with historical earthquake events, but finding damage assessment data for an area that suffered an earthquake with enough similarities to any study location would be difficult. More significantly, Geiß and Taubenböck (2013) confess that there is an absence of consistent definitions of key terms such as “risk” and “vulnerability” among researchers in the field. As a result, separate studies of similar scope and scale can have drastically different results, making it hard to decide which model would be the best one on which to base a disaster response.

One way to sidestep these concerns is to use a comprehensive modeling system with a standardized methodology that houses its own data. The Federal Emergency Management Agency (FEMA) has implemented such a system that is capable of running efficient models of major disasters throughout the United States. Called HAZUS-Multi Hazard (MH), the application works in conjunction with ArcGIS software and can be

used by any GIS professional or government organization that is interested in understanding how disasters such as earthquakes, floods, and hurricanes could impact their communities (FEMA 2014). FEMA works in partnership with the National Earthquake Hazards Reduction Program (NEHRP), creating and sharpening strategies to better prepare the United States for earthquakes (NEHRP 2014). This collaboration relies heavily on HAZUS-MH to achieve their stated goal of reducing loss of life and property damage due to earthquakes.

The database that is included with HAZUS-MH contains the best available engineering information for buildings (HAZUS-MH 2013). Also included is demographic data to analyze physical, social and economic losses from earthquakes (FEMA 2014). Thousands of historical earthquakes for the United States are included in the data so researchers could try to see what damage a subsequent earthquake would cause. HAZUS-MH can also accept outside data input so more experienced GIS users can analyze losses with more trusted and detailed information that they may possess. HAZUS-MH outputs include maps, charts, and reports that can convince any state, county or municipality to support and implement important safeguards in case a disaster strikes.

HAZUS-MH is a fascinating tool for disaster modeling and it can fill many needs when crafting the right emergency plan for any place, but it can be improved upon. HAZUS-MH is only equipped to model losses at a census tract level or larger. This poses a problem for modeling an earthquake scenario of casualties for many densely populated urban areas, where more detailed losses at a census block group level, census block level or even a parcel level would be desirable. These higher resolution levels help

find the way the casualties are distributed by units contained in the census tract. Though GIS professionals can generally overcome this limitation in the standard HAZUS-MH application by introducing additional data input such as more detailed building characteristics and demographic distribution, novice users would struggle with obtaining better data or know how to leverage the data in HAZUS-MH if they did have it available. Hopefully there would be an opportunity for less experienced users to apply this useful methodology to demographic data not already tied into the application.

1.2 Literature Review

This section contains a full literature review of related studies of estimating earthquake damages. Many studies of earthquake vulnerability utilized GIS software for analysis (Sahar, Muthukumar and French 2010, Hashemi and Alisheikh 2011, Aydoğan and Maktav 2009); several of which cited HAZUS-MH as a part of their process (Remo and Pinter 2012, Ploeger, Atkinson and Samson 2010, Neighbors et al. 2013). As this thesis explores estimating casualty counts, a review of population estimation studies have also been included here.

1.2.1 Earthquake Studies Using Remote Sensing – Light Detection and Ranging (LiDAR)

The use of Light Detection and Ranging (LiDAR) remote sensing technology has become increasingly popular in mapping the earth's surface. The process involves using a laser scanner attached to an aircraft that is aimed at the ground. The scanner shoots millions of laser pulses to determine an accurate depiction of the topography of the land below (and typically include tree canopies, buildings and other large objects). Figure 1 shows what a LiDAR scan of an urban area would look like. The calculation of the time

it takes for each pulse to travel to the surface of the earth and back to the source is then converted to elevation figures for the surface (Campbell and Wynne 2011, 245).

LiDAR data holds several uses for studying urban environments. Sampath and Shan (2007) used a modified convex hull approach to trace building footprints from LiDAR data in multiple urban settings. They documented how point spacing (resolution) of the LiDAR datasets and other factors such as building angles affected the regularization process that led to errors in the final output. Barazzetti, Brovelli and Valentini (2010) introduced a method that uses LiDAR data to correct errors inherent to aerial photos, including vertical displacement. Their results showed promise, especially for working with orthophotos of urban areas where tall buildings often distort the image.

Other types of remote sensing have been proven to demonstrate effective analysis of earthquake damage and vulnerability. Two examples are comparing pre- (5 meter

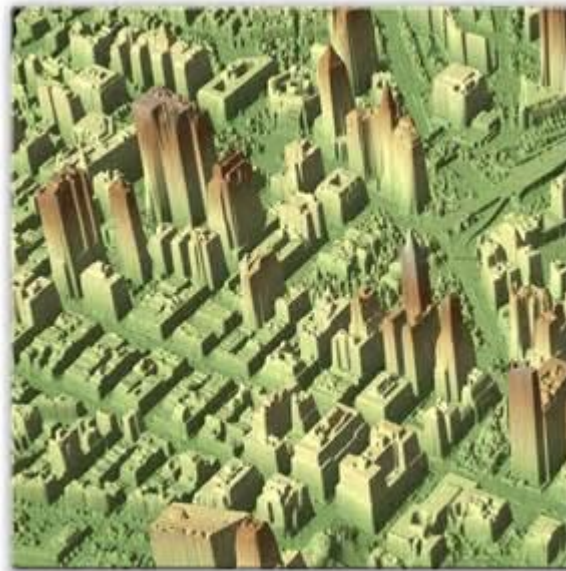


Figure 1 LiDAR Image of Urban Area
Source: http://oginfo.com/images/lidar_2_610.png
Accessed 15 April 2014

resolution) and post-earthquake (2.5 meter resolution) SPOT-5 panchromatic satellite images to recognize damaged structures (Dell'Acqua and Gamba 2012) and the use of radar-based tools to analyze changes in digital elevation models (DEM) of landscapes affected by an earthquake (Geiß and Taubenböck 2013, Liu et al. 2012). Despite its growing popularity, LiDAR has not had much utilization in earthquake damage and vulnerability studies. One possible reason for this is the ability to easily transform general building stock data as a substitute input. Hashemi and Alisheikh (2011) demonstrated this by using building stock data of a district in Tehran, Iran and making 3D images of each structure based on the number of stories for earthquake analysis. Fragility curves were created from the building materials data of the structures within the study area and a model was implemented to try to predict building damage, casualty counts and street blockages in the event of an earthquake occurring on the Mosha Fault nearby. The model was verified by analyzing actual damage and casualty data from the massive earthquake that damaged much of the city of Bam, Iran in 2003. Since there was not a good database available for Bam as there was for the district of Tehran, the results of the comparison were questionable. The upside was that the model does still identify likely points of destruction and street blockage, which can still contribute to working toward mitigating losses in case of an actual earthquake.

1.2.2 Earthquake Studies Using GIS: HAZUS Application

One feature of HAZUS-MH is the ability to supply supplemental data for earthquake loss analysis, giving users opportunities to compare results between their own data and what is already included when scenarios are played out. Remo and Pinter (2012) tried multiple soil maps to help predict losses for a potential large earthquake in

southeast Illinois. Their studies consistently showed that HAZUS-MH data overestimated damages and casualties compared to user-supplied data. Ploeger, Atkinson and Samson (2010) ran a HAZUS-MH model on potential damages that would occur if a strong earthquake were to strike near Ottawa, Canada. Despite extra steps required to overcome using an application designed for the U.S. in an international setting, the study helped identify areas of the city center that could receive the most damage from an earthquake. Moffatt and Cova (2010) used parcel data for all of Salt Lake County, Utah to try to predict economic loss estimates for each residential unit under a potential earthquake threat. They found that this was a massive undertaking given the amount of data involved. HAZUS-MH alone was not sufficient to run the analysis, so they used an alternate software package using the same methodology. The large scope of the project (almost 250,000 parcels analyzed) required additional computer hardware and scripting tools so the modeling could be completed in a reasonable amount of time.

Historical earthquakes can also be modeled in current times with HAZUS-MH. Neighbors et al. (2013) took this approach and analyzed both HAZUS-MH and user supplied data for a handful of earthquakes that occurred around King County, Washington in the past several decades. Again, HAZUS-MH supplied data overestimated losses compared to datasets brought in from outside sources. Kirscher, Whitman and Holmes (2006) used actual reported losses from the 1994 Northridge, California earthquake to see how close HAZUS-MH could estimate those losses. Though deaths were overestimated and serious injuries were underestimated, many of the estimated economic losses lined up closely to reported residential insurance claims that were paid.

1.2.3 Population Estimation Studies

Much like building vulnerability prediction, remote sensing is useful for population estimation studies. Dong, Ramesh and Nepali (2010) used ordinary least squares (OLS) regression methodologies to predict populations in Denton, Texas. Light Detection and Ranging (LiDAR) remote sensing data provided footprints and building heights and parcel data was used to filter out non-commercial and non-residential areas. Landsat TM was also included and helped establish land use for this study. Many of their estimations turned out to be lower than actual numbers as issues like spatial resolution discrepancies between LiDAR and Landsat and difficulty distinguishing between trees and structures in the LiDAR that was used caused some error. Qiu, Sridharan and Chen (2010) also looked at OLS for their population estimation study in Round Rock, Texas. Due to spatial autocorrelation leading to a higher incidence of Type I error, they opted to compare those results to spatial autoregressive models and witnessed a big improvement in their estimations. Silván-Cárdenas et al. (2010) tested four different algorithms on their remote sensing data to detect buildings and several methods of land use classification for areas of Austin, Texas. Their resulting population estimations suggested that overall accuracy assessments using the methods tested would improve if bias from estimated building attribute information were reduced.

Some of the same strategies used on these studies can also be applied to estimating the number of workers in an office building. Knowing these counts would be particularly useful for studying earthquake casualty counts in urban areas given the event takes place in the daytime. One such study conducted by Miller (2012) looked at trends of the amount of office space that is needed for each worker and breaks down some

estimations of office space per worker for many U.S. cities in addition to breakdown by various industries. This study did not utilize GIS; however, it gives important insight into developing a formula to calculate office worker numbers for buildings contained within a study area.

1.3 Research Question and Objectives

How effective would be the estimate of earthquake casualty counts obtained at a census block level for a downtown business district if the event took place during the daytime, when the study area contains the highest population count? HAZUS-MH methodology was used as a comparative tool for the Urban Daytime Seismic Casualty Estimation (UDSCE) customized application process using locally-sourced spatial data such as Light Detection and Ranging (LiDAR) data, parcels and property valuation assessor (PVA) data to generate all of the individual building parameters necessary to assess the overall vulnerability of each building. The UDSCE method is a newly built model designed to predict the distribution of estimated casualties in an urban environment. In a controlled scenario, the comparative analysis between HAZUS-MH and the UDSCE method was used to achieve the following measureable objectives:

- validation of the UDSCE method at the census tract level through comparison with the HAZUS-MH model results;
- higher resolution analysis using the UDSCE approach at a census block level;
- comparison of the UDSCE results at census tract, census block and parcel level.

The remainder of this thesis is divided into four chapters. Chapter 2 describes the study area in great detail and the importance of selecting this particular area for the stated objectives. Chapter 3 details the HAZUS-MH methodology and data that is included,

then introduces the UDSCE method and the data input used for the comparative analysis. Chapter 4 reports the findings of the spatial distribution of casualties by census block using the UDSCE method and identifies how it differs from the results of the census tract test are reported. Chapter 5 points out which areas of the study went well and which did not work, and it debates whether the UDSCE approach can be considered as an improvement over the current HAZUS-MH model.

CHAPTER 2: STUDY AREA AND SEISMIC HISTORY OF AREA

Chapter 2 introduces the study area and provides a brief discussion of past seismic events that occurred near the study area as a context for this study.

2.1 Study Area

The Central Business District (CBD) of Lexington, Kentucky has been selected as the study area for this experiment. The area is defined by 52 census blocks containing a total of 345 parcels that were analyzed for earthquake casualties under the UDSCE

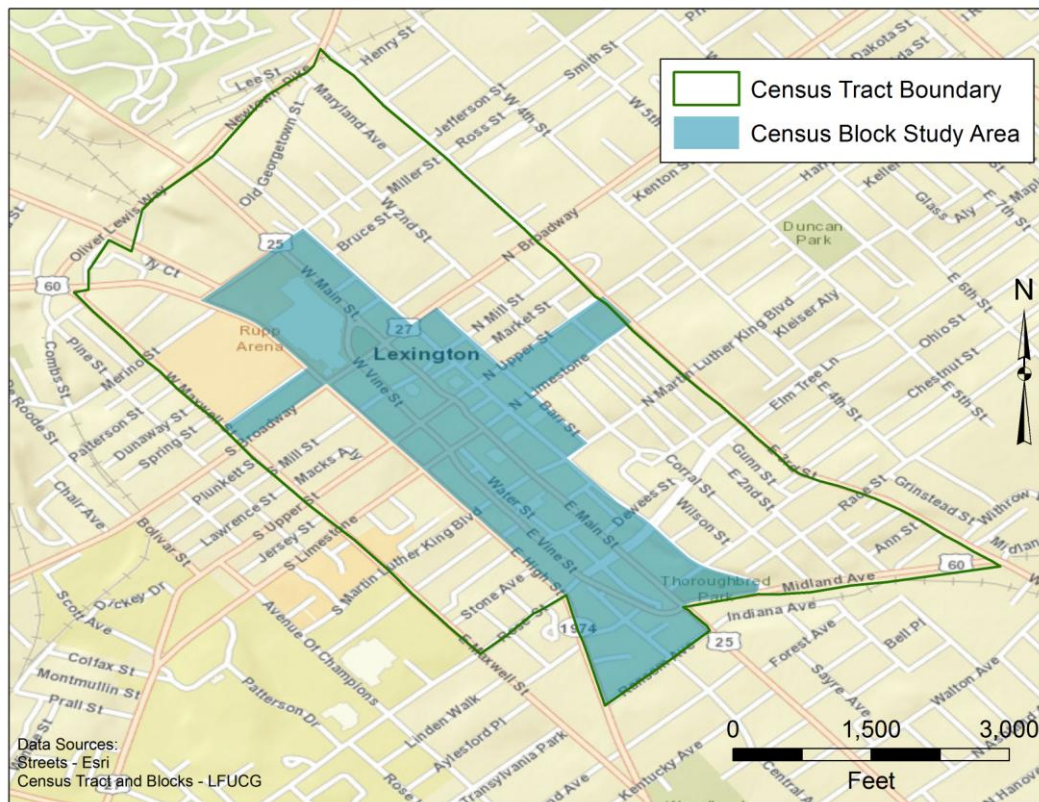


Figure 2 Study Area Map
Data Sources: Esri and LFUCG

method. Figure 2 illustrates the census block study area plus the boundary of census tract #21067000100, with a commercial working (daytime) population of 10,713, according to the 2000 census survey (U.S. Census 2013). This is the most current estimation of office workers available for this area and is already included with the data available to users of HAZUS-MH.

2.2 Seismic History of the Study Area

Lexington is not known for seismic activity, but its residents could be in more danger than most people realize. This section summarizes the history of notable earthquakes that have affected the state of Kentucky, including zones in neighboring states where future activity can still cause major damage for hundreds of miles around.

2.2.1 New Madrid Seismic Zone (NMSZ)

The NMSZ in southeast Missouri is the location of one of the largest earthquakes in U.S. history. A series of earthquakes occurred over the winter months of 1811-1812 along the NMSZ that devastated the sparsely populated region and disrupted the flow of the Mississippi River for several days. Each quake was believed to be in the magnitude range of 7.5 – 8.0, and one tremor caused church bells to ring 1,000 miles away in Boston (CUSEC 2013). Damage was reported in other faraway places, including Washington, D.C. and Charleston, South Carolina.

Scientists state that the probability of a magnitude 6.0 or higher earthquake occurring here in the next 50 years is between 25-40 percent (CUSEC 2013). An event of that magnitude happening again along the NMSZ would affect a much larger

population base that is not accustomed to dealing with seismic activity. The metropolises of Memphis, Tennessee and St. Louis, Missouri would be particularly vulnerable to large numbers of casualties as a result of future events in this zone. Lexington is located 400 miles to the northeast of the NMSZ, but the city is not far enough away to escape danger if future activity here is as strong as or stronger than the events of 1811-1812.

2.2.2 Wabash Valley Seismic Zone

The Wabash Valley Seismic Zone (WVSZ) is found along the Illinois-Indiana border where the Wabash River serves as the dividing line between the two states. Some recent moderate earthquakes centered within the zone have resulted in damage to structures in the state of Kentucky. A 5.2 magnitude earthquake centered near Mt. Carmel, Illinois on 18 April, 2008 was reviewed by Remo and Pinter (2012) in their HAZUS-MH study. This tremor caused a brick façade to collapse in Louisville, Kentucky, 150 miles to the east, but no injuries were reported in the state (The Business Journals 2008). A 5.4 magnitude earthquake that took place on 9 November, 1968 in the area did significant damage to the masonry of the City Building in Henderson, Kentucky, 50 miles away (USGS 2014).

The WVSZ is much closer to Lexington than the NMSZ at a distance of 250 miles. Recent history shows that it has been much more active as well. Though recent earthquakes in the WVSZ have not been as strong as what its counterpart has been known to produce, the possibility remains that this area is capable of stronger earthquakes in the future. Geologist Steven Obermeier found evidence of liquefaction (the process of seismic shaking turning soil into a substance similar to quicksand) within the zone in the

mid-1980's and believes that it was caused by an earthquake about 6,100 years ago at the estimated magnitude of 7.1 (CUSEC 2013).

2.2.3 Earthquakes and Faults Near the Study Area

Earthquakes that originated in the state of Kentucky were rarely moderate or strong in magnitude. Many of these tremors happened in the western half of the state, which were closer in proximity to the NMSZ and the WVSZ and were most likely not felt in Lexington. However, sporadic seismic activity has been observed in the northeastern part of the state for the last 150 years (Mauk, Christensen and Henry 1982). It was in this region where the state's strongest earthquake occurred. The event took place near Sharpsburg on 27 July, 1980, a mere 40 miles to the northeast of Lexington. This tremor measured 5.2 on the Richter scale and caused \$3 million worth of damage (\$8.4 million today) to hundreds of homes and businesses in and around the city of Maysville, 60 miles from Lexington (Street 1982).

Earthquake faults do exist in the immediate area around Lexington. The best visual evidence of fault lines are found along the Kentucky River fault system (KRFS). This system of fault lines run primarily east-west across the state of Kentucky, and gets as close as 15 miles to the CBD of Lexington (Vanarsdale 1986). Figure 3 shows the location of the KRFS and other fault lines in relation to the city of Lexington (LFUCG 2013).

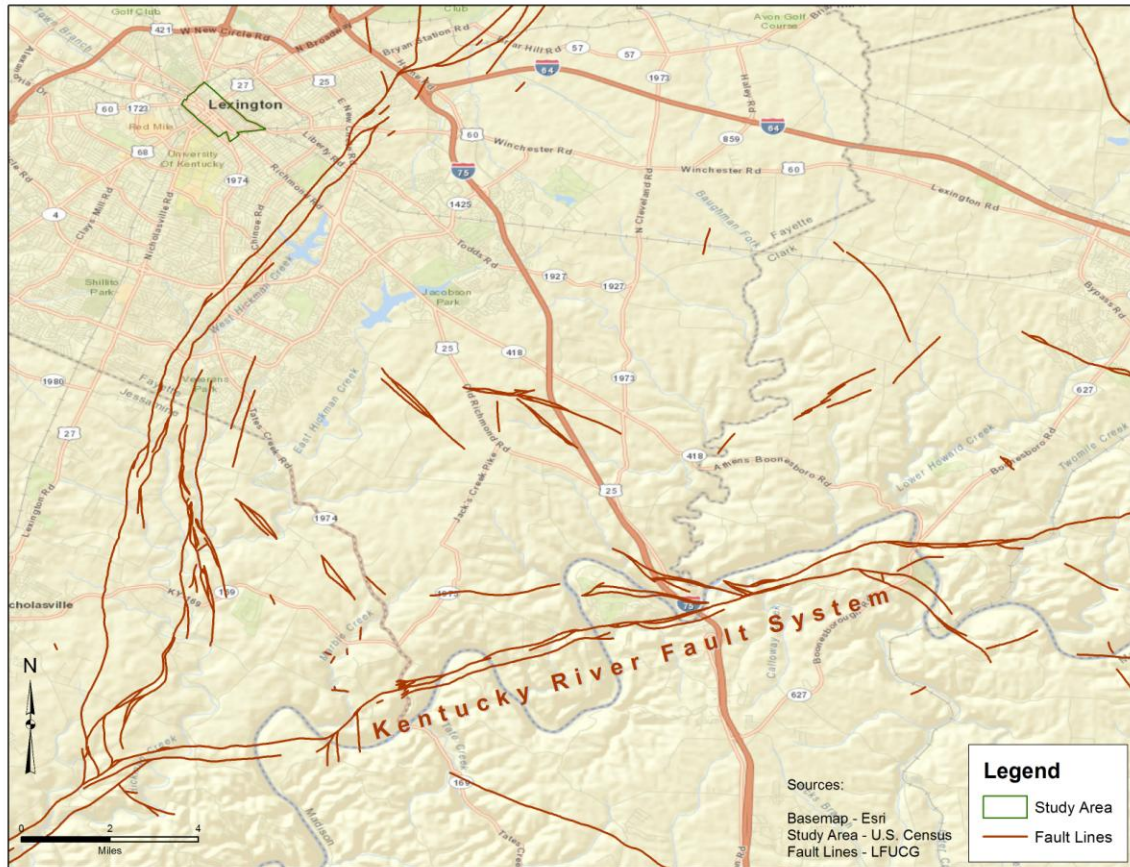


Figure 3 Map of Fault Lines in Central Kentucky
Data Sources: Esri, U.S. Census and LFUCG

CHAPTER 3: DATA SOURCES AND METHODOLOGY

Chapter 3 introduces the data types, sources, and pre-processing required for them to be used in this study. This is followed by the methodology subsection, which outline in detail the HAZUS-MH and UDSCE methods for earthquake casualty estimations used for this study.

The workflow followed in this study is summarized in Figure 4. This workflow outline the HAZUS-MH and UDSCE earthquake casualty models, the validation process of the results of the UDSCE versus HAZUS-MH models and relative percentage difference error estimation, the final steps in the UDSCE’s higher level casualties

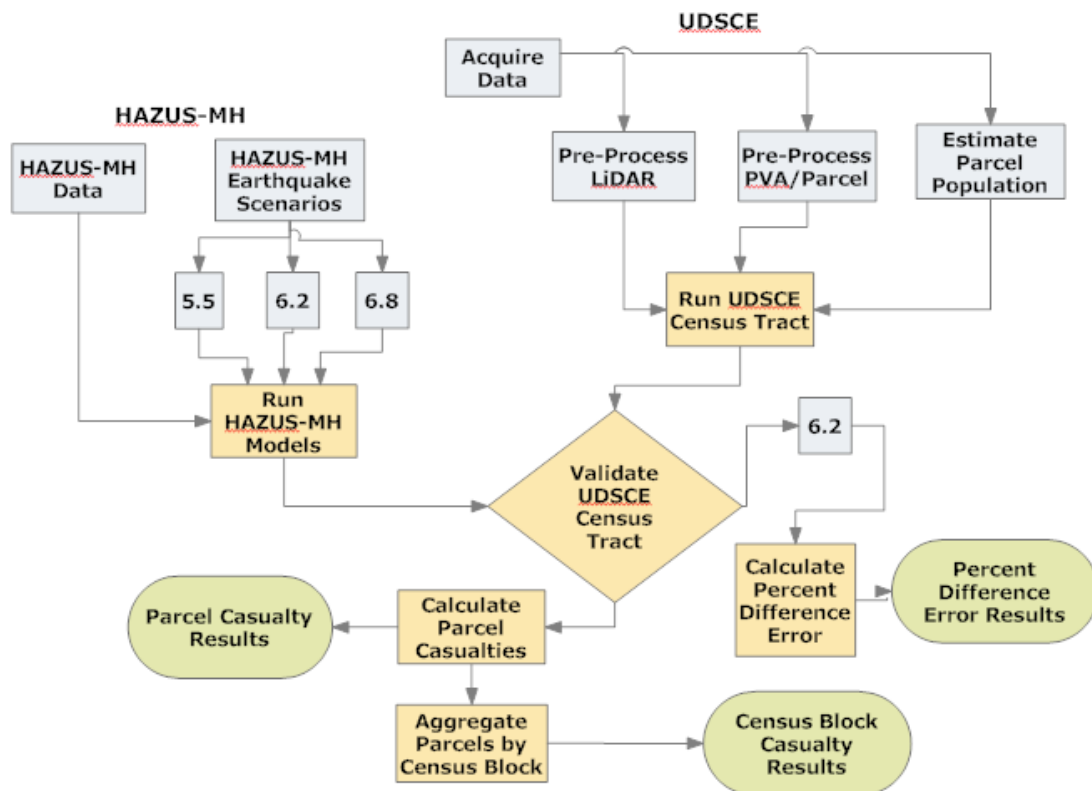


Figure 4 Workflow of Earthquake Casualty Estimation

computation at block and parcel level.

The HAZUS-MH component used (model defaults) building and population input and three earthquake magnitude scenarios to produce output used for the validation process. For the UDSCE component the input data were acquired specifically for this study and pre-processed, then a scoring method using three parameters of the structure (building height, age and material) was used to determine the building's vulnerability similarly to HAZUS-MH used standards. The UDSCE's results were validated by comparison with HAZUS-MH's output from three earthquake magnitude scenarios, finally the percentage difference error of the results was computed. Further analysis was then conducted with the UDSCE method to estimate casualties at higher resolution, specifically for block and parcel level.

3.1 Data Sources

The data used in this study are divided in three main categories encompassing census, LiDAR and parcel data. The sources, characterization, and importance of each data category in relation to this study will follow in this section.

3.1.1 Census Data

Census data were used to derive, with good accuracy, the number of people that reside in a multitude of geographic units such as states, counties and zip codes. Finer levels of resolution of census data such as census tracts and census blocks contain precise population and demographic data for studies of urbanized areas. The census block shapefile was publicly available through the U.S. Census website (U.S. Census 2013).

Table 1 Census Data Specifications

Dataset	Type/Format	Source(s)	Notes
Census Blocks	Vector polygon shapefile	U.S. Census	Resolution level for casualty estimation
Census Tract	Vector polygon shapefile	HAZUS-MH (created by U.S. Census)	Daytime population count for study area

The census tract used for the study was also created by the U.S. Census and was accessed through the HAZUS-MH application (HAZUS 2013). The census tract containing the study area estimates the daytime population for the area, which was critical to help calculate casualty counts for the study. Table 1 summarizes the census data used.

3.1.2 LiDAR Data

For this study, it was necessary to find the building heights associated with each parcel as this parameter is a component in determining earthquake vulnerability in buildings under the UDSCE method. The LiDAR files that were used for this study was created by Photo Science, Inc. in 2012 and was obtained for free through the Kentucky Geological Survey (KGS 2013). The data has a resolution of one meter, representing the spacing of the points during data collection (Table 2).

Table 2 LiDAR Data Characteristics

Dataset	Type/Format	Source(s)	Resolution	Year Created	Notes
LiDAR	Raster file (.las)	Kentucky Geological Survey (created by Photo Science, Inc.)	1 meter	2012	Building heights

3.1.3 Parcel and Ancillary Data

Parcel data and other ancillary datasets used in this study are summarized in Table 3. The Lexington-Fayette Property Valuation Administrator (PVA) office is responsible for assessing property values for the city of Lexington. The organization maintains a detailed parcel database that includes relevant information needed to analyze the response of buildings during an earthquake. Two building parameters required in the UDSCE method were the building material and the year the structure was built. This source also provided the two indicators in estimating the daytime populations of each parcel: the office square footage and land use. The PVA office provided an Excel spreadsheet of all parcels with these parameters for the central business district (CBD) of Lexington for a small fee (Lexington-Fayette PVA 2013).

A GIS parcel layer was also needed to represent the PVA information in a map. The parcels shapefile was created by and publicly available from the LFUCG's GIS website (LFUCG 2013). This shapefile contained a Parcel ID number that is also found

Table 3 Parcel and Other ArcGIS Data Specifications

Dataset	Type/Format	Source(s)	Notes
Land Use	Vector polygon shapefile	LFUCG	Land use of parcels within census tract not in study area
PVA Data	Excel spreadsheet	Lexington-Fayette PVA office	Material and year of structures
Parcel	Vector polygon shapefile	LFUCG	Location of buildings
Streets	Vector line shapefile	LFUCG	Mapping results

on the PVA spreadsheet. The merger of the parcel shapefile and the PVA spreadsheet shaped the final study area of block groups within the census tract that would be analyzed for casualty estimations.

Two ancillary datasets, a street shapefile and a land use shapefile were also obtained from the LFUCG GIS website (LFUCG 2013). The land use shapefile was used to identify land use for areas within the study census tract that was outside of the final study block area, thus to help refine the daytime population estimations. The street shapefile has been used as a context to enhance the mapping results.

3.2 Pre-processing Data

Each of the acquired datasets for this study required preprocessing steps before the data could be used. This section describes in detail the preprocessing for each dataset.

3.2.1 Census Pre-processing: Estimating Daytime Populations By Parcel

An important element required for the UDSCE analysis was to calculate daytime populations by parcel, for each office building within the study area, from the census data. For this purpose, an average number of square feet of office space per worker was considered and used in the UDSCE method. Figure 5 displays the office square footage for both the study area and the territory outside of the study area within the census tract (Lexington-Fayette PVA 2013). The average office space utilized per worker in this scenario was 351.16 sq. ft., where 92.5 percent of the office space within the census tract lies in the study area, as shown in Table 4. Using the 2000 U.S. Census figure of daytime

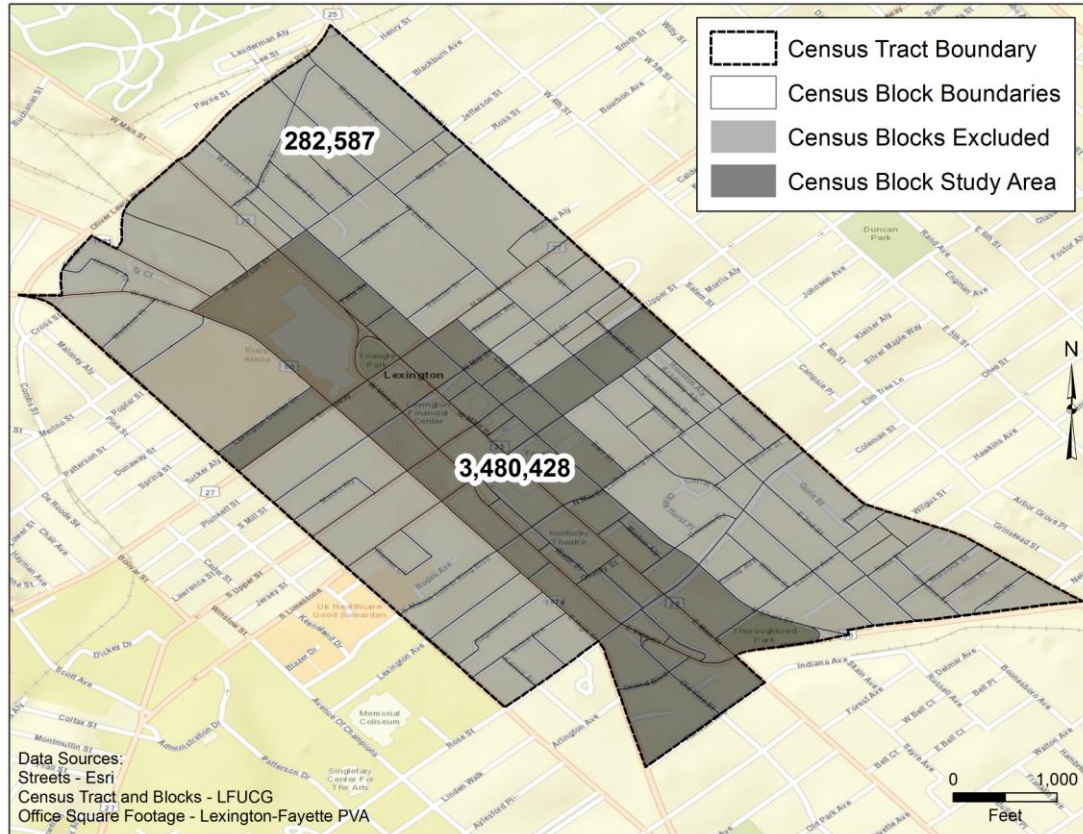


Figure 5 Map of Office Square Footage For Census Tract
Data Sources: Esri, LFUCG (2013) and Lexington-Fayette PVA (2013)

commercial population of 10,716 for the entire census tract, the total office workers within the study area was calculated at 9,912.

As no reliable retail or visitor daytime populations were available for the study, the 351.16 sq. ft. per person average was also applied to the retail and hospitality/recreation designated parcels. This process added 5,452 people to the total daytime population for the study area. Most residential parcels within the study area were ruled out, based on the assumption that people would not likely be at their residence in the middle of the day. The two exceptions made were for parcels containing a large apartment complex. Based on their size, they were given default daytime population

Table 4 Breakdown of Office Worker Population for Census Tract

Census Blocks	Office Worker Population	Office Sq. Ft.	Percent Total	Avg. Office Space/Worker
Within Study Area	9,912	3,480,428	92.5	351.16
Outside of Study Area	804	282,587	7.5	351.16
Totals	10,716	3,763,015	100	351.16

Sources: U.S. Census (2013), Lexington-Fayette PVA (2013)

values of 100 and 50. Other land use categories that were ruled out due to the assumption of the daytime scenario were vacant lots, parking structures and church parcels.

3.2.2 Pre-processing LiDAR Data

The LiDAR data were used to derive the building height within each parcel of the study area. Since the input LiDAR file (.lsa format) is not compatible with ArcGIS, the conversion tool .lsa file to multipoint data file, available in ArcGIS 10.2, was employed to convert the data. This conversion resulted in a large multipoint data file covering the entire area. Then, only the points within the final study area (represented by the area in dark gray in Figure 5) were extracted using the clip tool. The raw LiDAR data for the study area are shown in Figure 6.

The z-values (representing elevation) were then extracted from the clipped multipoint file and spatially joined to the parcel data. The point within each parcel with the highest z-value was used to establish the elevation for each parcel's building top. This practice was used assuming that only one building occupies each parcel within the study area. A new field was created for the parcel shapefile and populated by subtracting



**Figure 6 Raw LiDAR Points of Study Area
Overhead and Horizon View
Data Source: Photo Science, Inc. (2012)**

the known ground elevation value from the z-value to set each parcel's building height. The pre-processing steps for the LiDAR data are shown in the flowchart in Figure 7.

3.2.3 Pre-processing Parcel Data

Pre-processing of both the PVA spreadsheet and the parcel shapefile was necessary before the analysis. The flowchart of the required pre-processing steps is shown in Figure 8. First, the building information from the PVA spreadsheet was merged into the parcel shapefile. This was done by joining the shapefile and table in ArcGIS 10.2, using the Parcel ID number as the matching field for each one. This process selected only the parcels in the shapefile that had a match to the parcels in the PVA spreadsheet and added the square footage, building material and year of construction fields for those parcels, thus creating the final study area seen in Figure 9.

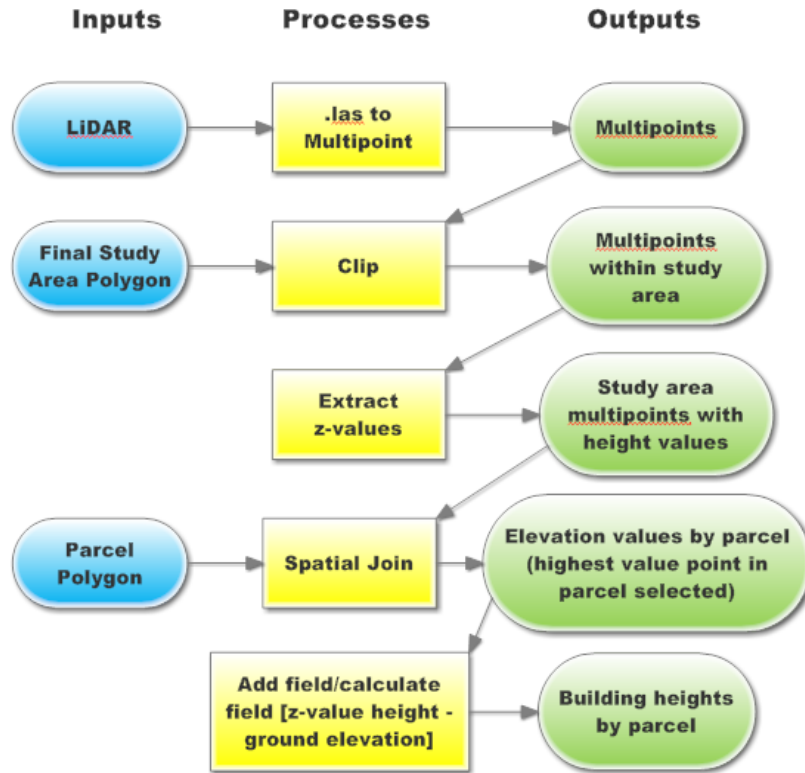


Figure 7 LiDAR Pre-processing Flowchart

3.2.4 Changes to Pre-processing Based on Study Area Data Acquisition

It should be noted here that the necessary three datasets used in the UDSCE method, specifically LiDAR, Parcel, and PVA, might be available in other format depending on the study area and relative data sources. Therefore, the steps outlined for the data pre-processing used in the UDSCE method may have to be altered and/or appended depending on the formats in which the data are. A summary of the potential alternate formats for each dataset used is provided in Table 5.

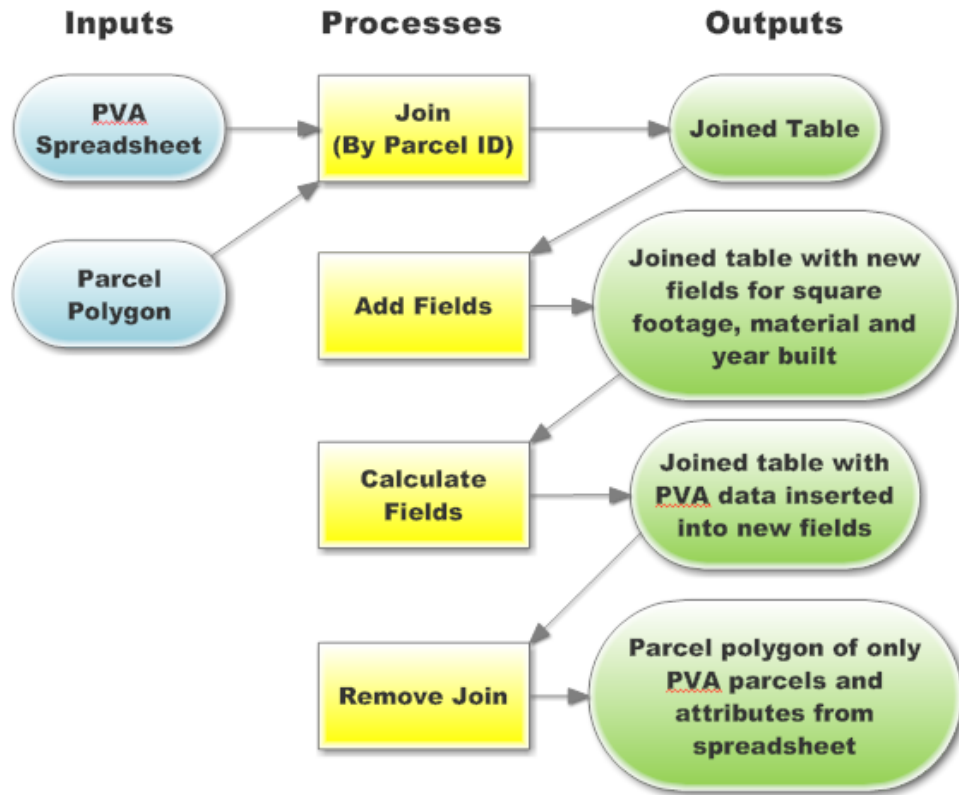
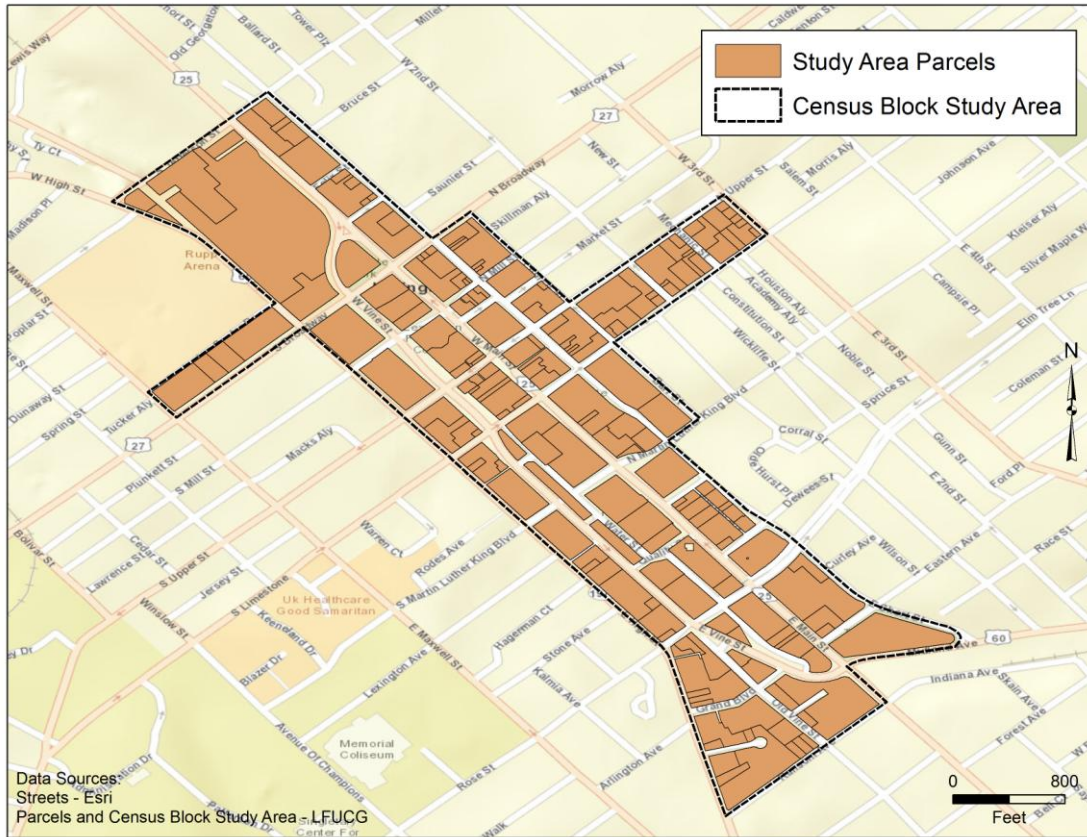


Figure 8 Parcel Pre-processing Flowchart

Table 5 Alternate Formats of Datasets Used For UDSCE Method

Dataset	Format Used	Alternate Format(s)	Notes
LiDAR	.las	None	Widely accepted; if not available for study area then other options should be explored to get building height
Parcel	.shp (Esri)	MapInfo and other GIS software formats	.shp is used with ArcGIS and is most common. MapInfo formats can easily be converted to .shp
PVA	.xls	ASCII	ArcGIS can work with any spreadsheet or database file that can match up with data in .shp format



**Figure 9 Map of Study Area Parcels
Data Sources: Esri, LFUCG**

3.3 Methodology

The methods used for this study are described by first focusing on how HAZUS-MH was used to determine casualties at the census tract level. Then the UDSCE method at the census tract level is described along with the validation process using the results of the HAZUS-MH at the census tract level. The details of the UDSCE method at census block level is then introduced with details on how it was adapted to estimate casualties at the census block level for the Lexington CBD.

3.3.1 HAZUS-MH Methodology

The HAZUS-MH application requires three input to run an earthquake casualty estimation. These input are the earthquake’s location of origin, magnitude and depth below the surface. HAZUS-MH then computes casualties for the selected study area, based on its population and building inventory. HAZUS-MH reports earthquake casualties at four levels of severity for injuries as shown in Table 6.

The event tree model of the basic HAZUS-MH process of earthquake casualty estimation at the census tract level is shown in Figure 10. The HAZUS-MH methodology for estimating earthquake casualties considers several factors using the supplied census data. One key factor is how the population is distributed in the study area. In Table 7 is illustrated the census population distribution as default setting used for this study (HAZUS-MH 2013). This chart is used to estimate populations indoors during the daytime earthquake scenario; the application has separate scenarios for nighttime (2 a.m.)

Table 6 Description of Injury Severity Levels for HAZUS-MH

Injury Severity Level	Injury Description
Level 1	Cuts, minor burns or any other medical issue that does not require hospitalization
Level 2	Broken bones, concussions or any other medical issue requiring hospitalization but not expected to be life-threatening
Level 3	Life-threatening injuries that must be addressed to prevent death such as spinal injuries or internal bleeding
Level 4	Instantaneously killed or mortally wounded

Source: HAZUS-MH (2013)

Table 7 HAZUS-MH Default Setting For Population Distribution

Occupancy	2 p.m. (Indoor)	Where:
Residential	$(0.70)0.75(DRES)$	DRES = daytime residential population
Commercial	$(0.99)0.98(COMW) + (0.80)0.20(DRES) + 0.80(HOTEL) + 0.80(VISIT)$	COMW = number of people employed in commercial sector HOTEL = number of people staying in a hotel VISIT = number of non-residents visiting for shopping, entertainment, etc.
Educational	$(0.90)0.80(GRADE) + 0.80(COLLEGE)$	GRADE = number of students in grade schools (K-12) COLLEGE = number of students attending college
Industrial	$(0.90)0.80(INDW)$	INDW = number of people employed in the industrial sector
Hotels	$0.19(HOTEL)$	First Multiplier = ratio of population indoors/outdoors Second Multiplier = ratio of population located at a particular occupancy for the scenario time

Source: HAZUS-MH (2013)

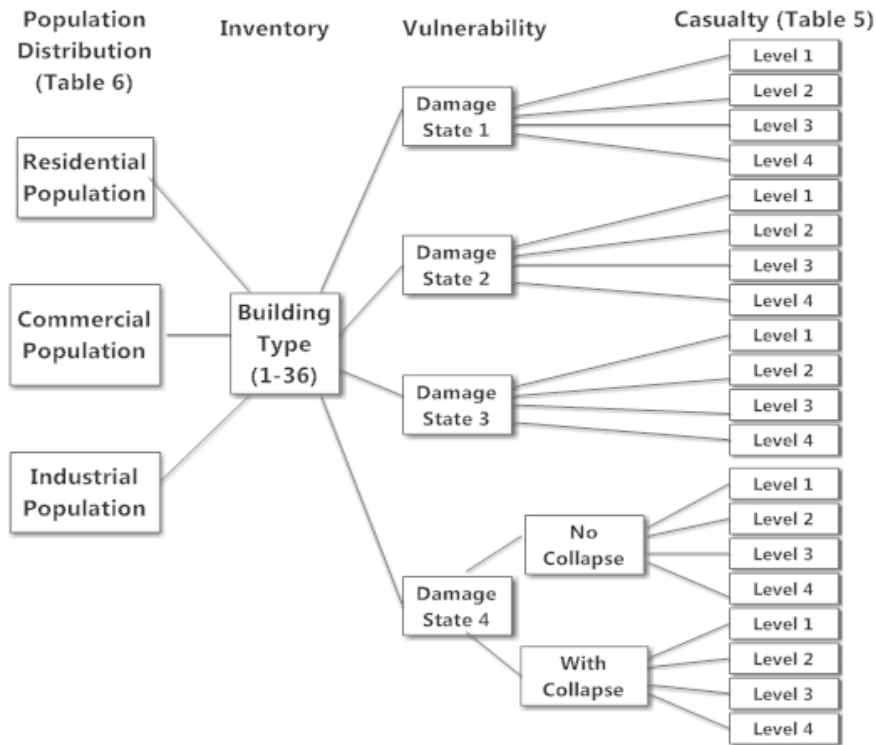


Figure 10 HAZUS-MH Earthquake Methodology Flowchart

Source: HAZUS-MH (2013)

and commute time (5 p.m.). Using the right scenario is important as the population is assumed not to be stationary over a 24-hour period. Another important assumption in HAZUS-MH relates to the ratio of the population that would be located indoors or outdoors during the earthquake in an attempt to better simulate a real-life scenario, thus leading to more accurate casualty counts. For this study, only indoor casualties were considered.

The other major input HAZUS-MH considers when estimating earthquake casualties is the building inventory contained in the application. The HAZUS-MH earthquake technical manual lists default casualty rates for 36 different building types for five damage states: slight, moderate, extensive, complete (non-collapse) and complete (collapse) (HAZUS-MH 2013). Each building type has a specific vulnerability to seismic activity based on type of construction, building materials and number of stories. The complete tables of these casualty rates by building type can be viewed in Appendices A through E.

3.3.2 UDSCE Method at Census Tract Level

The UDSCE method was developed in an attempt to simplify the HAZUS-MH method of estimating casualties in an urbanized area as the result of an earthquake occurring during the day. The UDSCE new methodology is outlined in Figure 11. This method allows for casualty estimations to be viewed at a census block level, improving upon the limitation of HAZUS-MH results at the census tract level. The foundation of the UDSCE method is the scoring process of three key building components: building height, age and material. The total scores are then grouped according to the damage

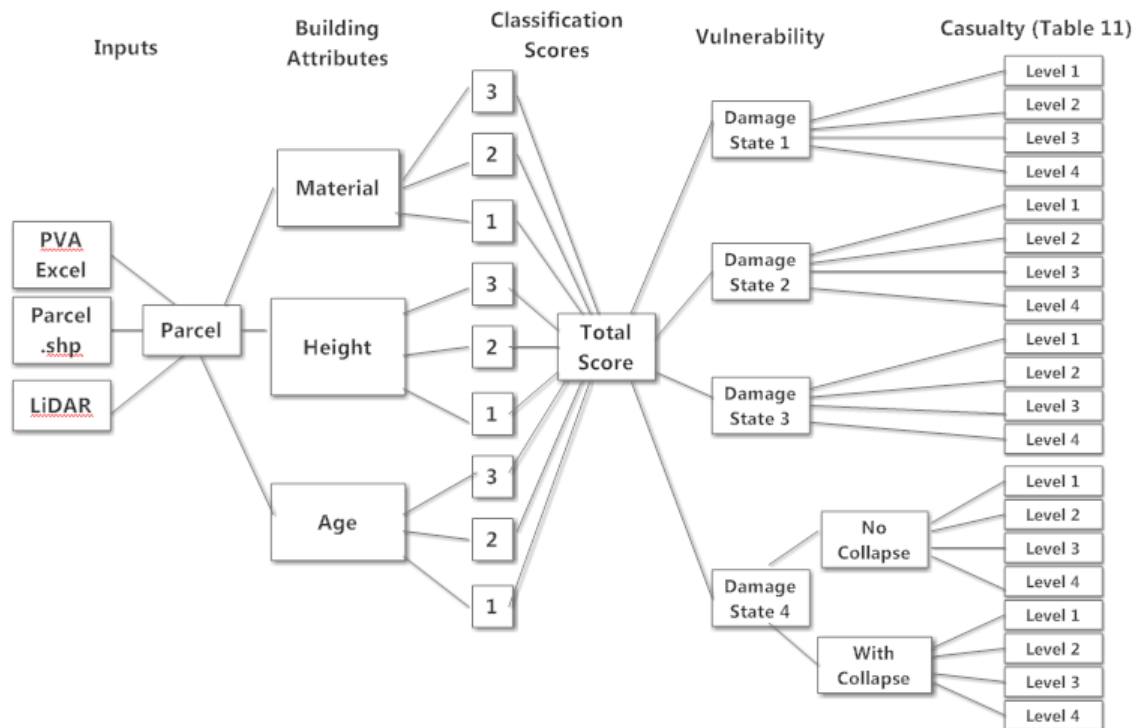


Figure 11 UDSCE Method Flowchart

states used by HAZUS-MH which yields the rates to calculate estimated casualties for each parcel. The rates are aggregated to the census tract level for comparison to the HAZUS-MH results for the given earthquake scenario. The following subsections explain how each attribute’s scores were determined, and how the total scores were classified.

3.3.2.1 Criteria for the UDSCE Building Material Score

The Lexington-Fayette PVA data indicated the building material of each parcel. Within the study area, 11 different building materials have been identified. These attributes were grouped into three classes based on vulnerability to seismic activity, as shown in Table 8. Ploeger, Atkinson and Samson (2010) summarized from their study

Table 8 Building Material Scores

Building Material Class	Score
Masonry & Frame Masonry & Metal Frame	3
Brick & Concrete Block Concrete Block Native Stone Brick Veneer	2
Glass Glass & Masonry Concrete Load Bearing Concrete Non-Load Bearing	1

observations vulnerability by building material, which forms the basis of the UDSCE building material score. Any structure containing a steel or wood frame received the highest score of “3”. Concrete and unreinforced masonry structures were much more likely to cause injuries and deaths, so they were given a score of “1”. Some structures contained glass and therefore were also categorized as a “1” for their fragility. Any other building type found in the study area that did not fit these two categories were given a score of “2”.

3.3.2.2 Criteria for the UDSCE Building Height Score

The LiDAR data provided information about the building heights for each parcel in the study area. This parameter is somewhat different for this study in that for previous studies the number of stories for each building was used instead of the height

Table 9 Building Height Scores

Height Range	Number of Stories	Score
Up to 100 feet	1-8	3
100-150 feet	9-12	2
Above 150 feet	13+	1

measurement. Güzey et. al. (2013) and Hashemi and Alisheikh (2011) each factored in number of stories in their respective building vulnerability studies, with higher storied buildings generally more likely to cause casualties in an earthquake as shown in Table 9. The HAZUS-MH application in most cases allocate 10 or 12 feet per story in their building classification methodology to determine the building’s approximate height. For this study, each building up to 100 feet [1-8 stories] in height received a score of “3”, buildings between 100 to 150 feet [9-12 stories] in height received a score of “2” and all buildings taller than 150 feet [13 or more stories] in height received a score of “1”.

3.3.2.3 Criteria for the UDSCE Building Age Score

The age of the structures play a part in its vulnerability to earthquakes. The HAZUS-MH application classifies structures by four different levels of code: high-code, moderate code, low code, and pre-code (built before seismic standards). The year built is a large factor in this designation, but to a smaller degree and so is the region of the country the building is located (HAZUS-MH 2013). Putting the year built attribute from the Lexington-Fayette PVA data into year ranges of vulnerability was done for this study as summarized in Table 10. The lowest score of “1” was assigned to structures built

Table 10 Building Age Scores

Year Built Range	Score
1980 - Current	3
Between 1940-1979	2
Before 1940	1

before 1940, since no seismic codes existed before this date. For any structure built between 1940 and 1979, a score of “2” was designated, and a score of “3” was assigned to the buildings built in 1980 and later.

3.3.2.4 Criteria for the UDSCE Total Score

Each parcel’s score for building material, height and age was then added up for a total score. The total score represented what damage state the structure would fall and to which would be assigned the casualty rates among the four injury severity levels from the

Table 11 Total Score Ratings

Total Score	Damage State
8-9	Slight
6-7	Moderate
5	Extensive
4	Complete (No Collapse)
3	Complete (Collapse)

correlating tables found in HAZUS-MH (HAZUS-MH 2013). The resulting total scores are summarized in Table 11. Since the HAZUS-MH indoor casualty rate tables (HAZUS-MH 2013) have listings for 36 different building types, the most common rates found within each table were used for the UDSCE method. These rates are summarized in Table 12. Two examples of the computed scores predicting vulnerability and casualties can be seen in Table 13 and 14.

The ModelBuilder application in ArcGIS 10.2 was used to automate the process of calculating all new fields for both the scores and the associated casualty rates. A snapshot of the model can be viewed in Figure 12. The input StudyAreaParcels shapefile has already been pre-processed with the addition of the three parameters identified to predict vulnerability to seismic activity. By running this model, all necessary fields were created and populated by the criteria described, then the parcel casualty rates were aggregated.

Table 12 UDSCE Assigned Casualty Rates by Damage State

Total Score	Damage State	Casualties (%)				% HAZUS-MH Building Types Use
		Level 1	Level 2	Level 3	Level 4	
8-9	Slight	.05	0	0	0	100
6-7	Moderate	.20	.025	0	0	52.78
5	Extensive	1	.1	.001	.001	94.44
4	Complete (No collapse)	5	1	.01	.01	94.44
3	Complete (Collapse)	40	20	5	10	91.67

Table 13 Examples of Vulnerability Calculation by Parcel

Parcel ID	Address	Material	Material Score	Height (ft)	Height Score	Year Built	Year Score	Total Score	Damage State
14262300	152 Market St.	Brick Veneer	2	90	3	1950	2	7	Moderate
10130050	300 W. Vine St.	Concrete Load Bearing	1	319	1	1977	2	4	Complete (No Collapse)

Table 14 Examples of Casualty Calculation by Parcel

Parcel ID	Address	Damage State	Land Use	Sq. Ft.	Day Pop	Level 1 Cas	Level 2 Cas	Level 3 Cas	Level 4 Cas	TotCas
14262300	152 Market St.	Moderate	Comm	4148	12	0.024	0.003	0	0	0.027
10130050	300 W. Vine St.	Complete (No Collapse)	Comm	387597	1104	55.200	11.040	0.110	0.110	66.461

3.3.3 UDSCE Method at Census Block Level

Utilizing the UDSCE method at the census block level allows for a more precise localization of where casualties would likely be found within a census tract. The methodology, as shown in Figure 11, have been used for each parcel found within the study area census block. This change allowed for the casualty levels for each damage state to be aggregated by their corresponding census blocks. Also, with estimated daytime populations calculated for each parcel in the study area, the census blocks had the capability to be mapped by casualty counts as well as casualty rates. The ModelBuilder model of the UDSCE method for census blocks can be seen in Figure 13.

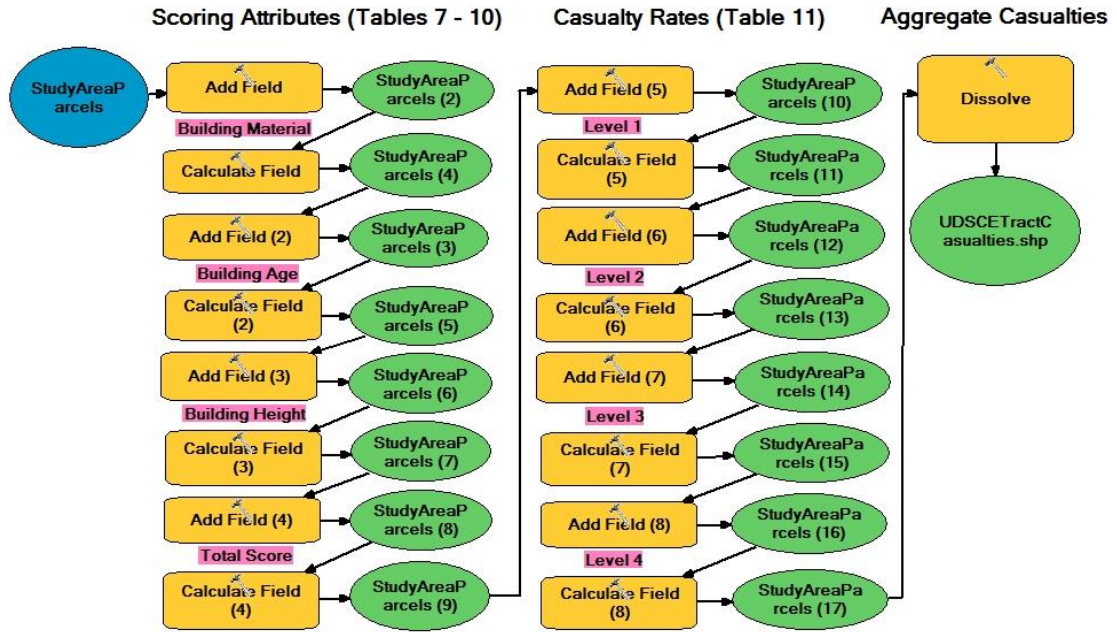


Figure 12 ModelBuilder Design of UDSCE Method by Census Tract

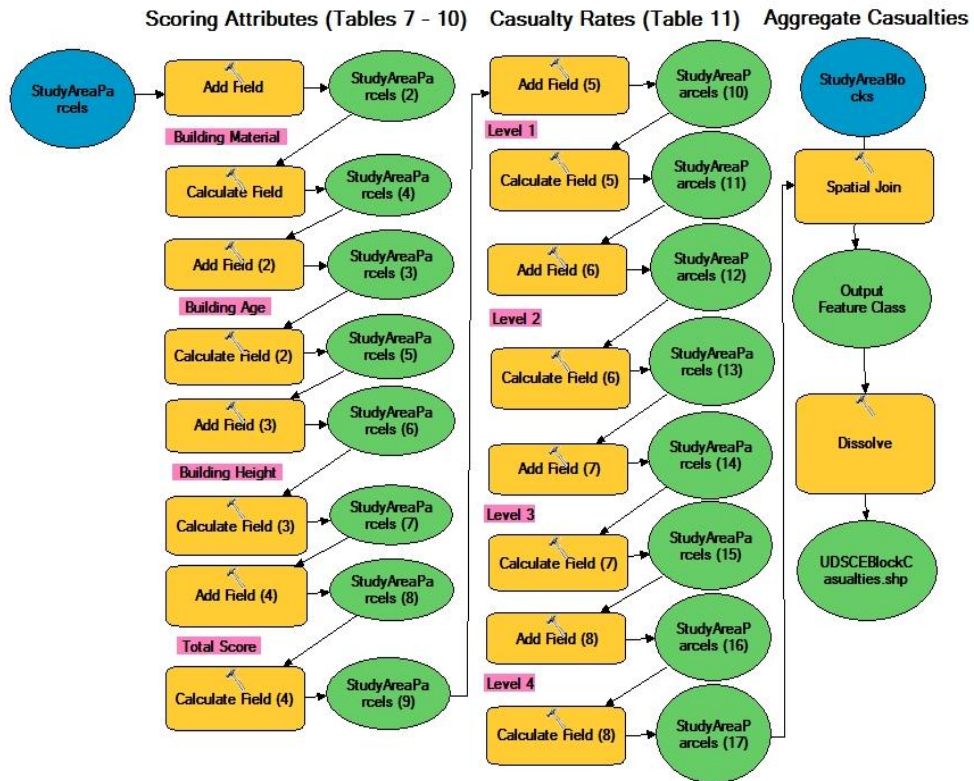


Figure 13 ModelBuilder Design of UDSCE Method by Census Block

CHAPTER 4: RESULTS

The epicenter location of an hypothetical earthquake along the Kentucky River Fault System was set in order to derive casualty estimates using the HAZUS-MH. Results were used to validate the results of the new UDSCE method and derive relative comparison of casualties results at census track, block and parcel resolution. The coordinates for the earthquake scenario were at 37.880332 degrees latitude and -84.369709 degrees longitude, which placed the epicenter approximately 13.5 miles to the southeast of the study area, as shown in Figure 14. The depth of the earthquake was set at 16.09 km (10

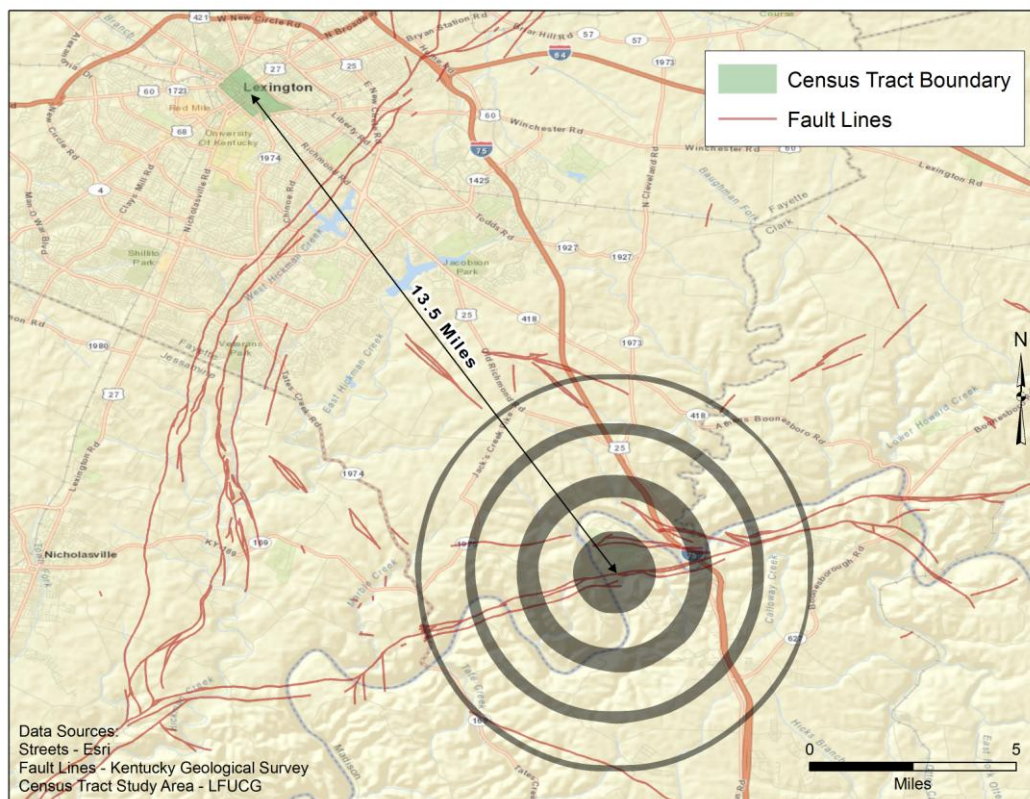


Figure 14 Map of Earthquake Epicenter
Data Sources: Esri, Kentucky Geological Survey, LFUCG

miles) below the surface, based on historical earthquake records documented in the area (Street 1982).

First the HAZUS-MH application was run with the determined epicenter input under three magnitude scenarios: 5.5 (Moderate 5-5.9), 6.2 and 6.8 (Strong 6-6.9). The classes are listed according to the Earthquake Magnitude Classes (UPSeis 2014). The recorded earthquake effects for the used magnitudes are:

2.5 to 5.4	Often felt, but only causes minor damage
5.5 to 6.0	Slight damage to buildings and other structures
6.1 to 6.9	May cause a lot of damage in very populated areas

This was done to evaluate at what strength the relative runs with the UDSCE method would best model the casualty counts at the census tract level. Then the UDSCE model was run, for the same scenario, at the census block level and parcel level to refine the casualty estimates at higher resolution.

4.1 HAZUS-MH Results

The results of the total casualty estimations from three separate magnitudes for census tract #21067000100 can be seen in Figure 15. The complete breakdown for each magnitude by severity level are summarized in Table 15, 16 and 17. These casualty estimates represent the 2 p.m. (afternoon) scenario only for people located indoors. Counts were broken down by the four severity levels as well as by building use. For the 5.5 magnitude scenario, the number of total injuries expected was 26, with one potential death. A total of 289 casualties were predicted under the 6.2 magnitude scenario, including 15 deaths. The 6.8 magnitude scenario calculated 730 casualties, of which 45 people lost their lives.

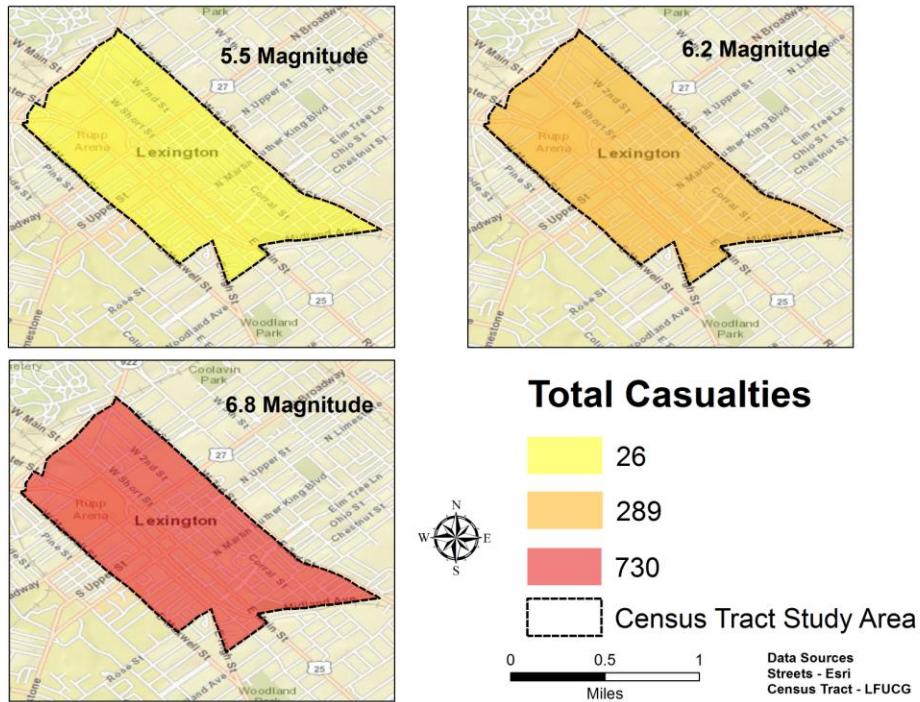


Figure 15 HAZUS-MH Total Casualty Maps by Magnitude

Casualties occurred primarily in the lower severity levels (1 and 2) and were found most often associated with commercial structures. This is not surprising as the census tract contains the CBD of Lexington and is largely made up of office buildings

Table 15 HAZUS-MH Casualty Estimates for 5.5 Magnitude Earthquake

Land Use	Severity 1	Severity 2	Severity 3	Severity 4	Total
Commercial	19	3	0	1	23
Educational	2	0	0	0	2
Hotels	0	0	0	0	0
Industrial	0	0	0	0	0
Other Residential	1	0	0	0	1
Single Family	0	0	0	0	0
Total	22	3	0	1	26

and retail outlets.

Table 16 HAZUS-MH Casualty Estimates for 6.2 Magnitude Earthquake

Land Use	Severity 1	Severity 2	Severity 3	Severity 4	Total
Commercial	188	51	7	14	260
Educational	12	3	1	1	17
Hotels	0	0	0	0	0
Industrial	5	1	0	0	6
Other Residential	4	1	0	0	5
Single Family	1	0	0	0	1
Total	210	56	8	15	289

Table 17 HAZUS-MH Casualty Estimates for 6.8 Magnitude Earthquake

Land Use	Severity 1	Severity 2	Severity 3	Severity 4	Total
Commercial	452	135	20	40	647
Educational	34	11	2	3	50
Hotels	0	0	0	0	0
Industrial	10	3	0	1	14
Other Residential	11	3	1	1	16
Single Family	2	1	0	0	3
Total	509	153	23	45	730

4.2 UDSCE Method at Census Tract Level Results

The results of the UDSCE method for determining total casualties from earthquakes are shown in Figure 16 while the complete breakdown by severity level is shown in Table 18. It is important to note that the UDSCE method was not designed to receive input of magnitude like HAZUS-MH but rather assigned casualty rates by damage state (Section 3.3.2, Table 11). These results are representative of the census block study area of parcels within the census tract, shown in Figure 9, rather than the entire census tract used for the HAZUS-MH studies. This extent was determined by the PVA spreadsheet of parcels covering only the entire census block study area. However,

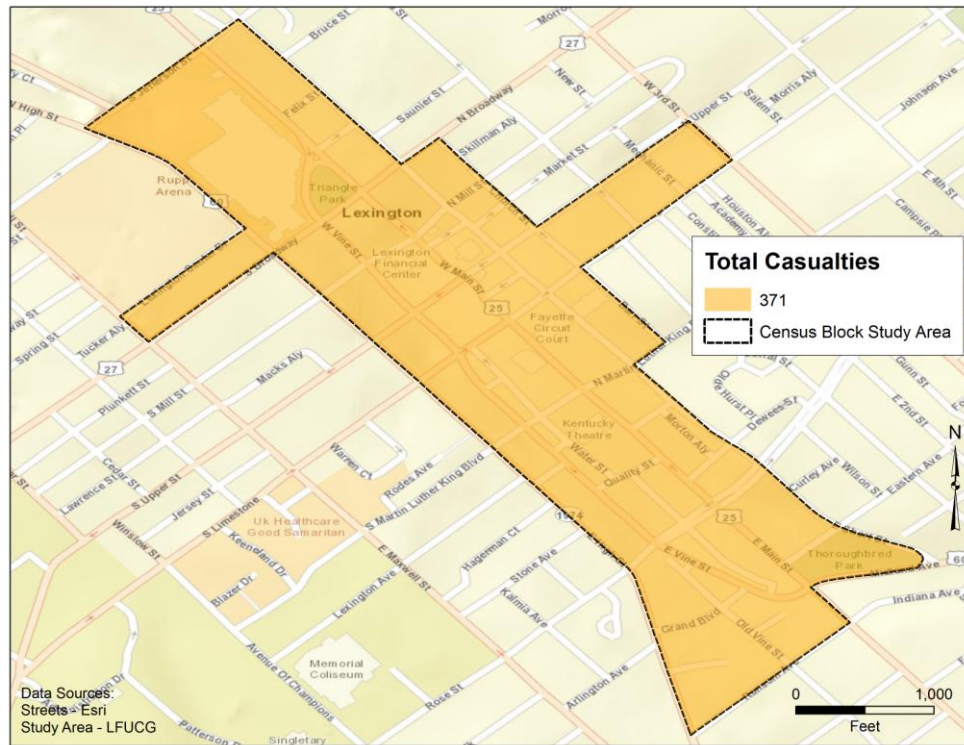


Figure 16 UDSCE Method Total Casualties in Study Area Map

as noted in Section 3.2.1, 92.5 percent of the CBD commercial space from the census tract is included in the census block study area, and the HAZUS-MH studies conducted show that this is where most of the injuries would occur. A total of 371 injuries for the census block study area were predicted under the UDSCE method, with the potential for one fatality.

Just like in the HAZUS-MH studies, injuries were on the lower levels of severity and most commonly associated with the CDB commercial structures. No injuries were expected with hotels or single family residences, as people typically do not occupy them during the early afternoon hours. Casualties from educational and industrial parcels were not evident in this case as no parcels within the study area fit either of these criteria.

4.2.1 Validation of UDSCE Method

In comparison to the HAZUS-MH predictions, the UDSCE method suggests that it is modeling earthquake casualties at multiple strengths based on the severity level. For

Table 18 UDSCE Method For Study Area Results

Land Use	Severity 1	Severity 2	Severity 3	Severity 4	Total
Commercial	303	57	1	1	362
Educational	0	0	0	0	0
Hotels	0	0	0	0	0
Industrial	0	0	0	0	0
Other Residential	7	2	0	0	9
Single Family	0	0	0	0	0
Total	310	59	1	1	371

total casualties, the UDSCE method has the closest ties to the 6.2 magnitude scenario from HAZUS-MH, as seen in Table 19. In contrast, the Severity 3 and Severity 4 levels of casualties predicted by the UDSCE method are much closer to the 5.5 magnitude prediction generated by the HAZUS-MH method, in which these levels of injuries are rare.

For a closer look at the differences in estimations between the three HAZUS-MH models and the UDSCE model, the Percent Difference Error (PDE) analysis was used (University of California, Davis 2014). This analysis can be used to compare model values, in this case the HAZUS-MH results and the UDSCE method results. In equation (1) the absolute value of the difference between the HAZUS-MH value (h) and the UDSCE value (u) divided by their average is multiplied by 100:

$$\frac{|h-u|}{|(h+u)/2|} * 100 \quad (1)$$

where: h = the HAZUS-MH result; u = the UDSCE method result.

The results of the percent difference error analysis are summarized in Table 20. A percentage difference error very close to zero means that the UDSCE model values are

Table 19 Comparison of HAZUS-MH and UDSCE Results

Method	Severity 1	Severity 2	Severity 3	Severity 4	Total
HAZUS-MH 5.5 Magnitude	22	3	0	1	26
HAZUS-MH 6.2 Magnitude	210	56	8	15	289
HAZUS-MH 6.8 Magnitude	509	153	23	45	730
UDSCE Method	310	59	1	1	371

Table 20 Percent Difference Error Analysis of Results

Method	Severity 1 (%)	Severity 2 (%)	Severity 3 (%)	Severity 4 (%)	Total (%)
HAZUS-MH 5.5 Magnitude	173.5	180.6	200.0	0.0	173.8
HAZUS-MH 6.2 Magnitude	38.5	5.2	155.6	175.0	24.8
HAZUS-MH 6.8 Magnitude	48.6	88.7	183.3	191.3	65.2

very close to the HAZUS-MH results and represented earthquake scenario. The PDE values outline that the UDSCE model results best match the casualties rates for the 6.2 magnitude earthquake scenario for both Severity 1, Severity 2 and Total, while overestimating the other values (Severity 3 and Severity 4).

4.3 UDSCE Method at Census Block Level Results

The results of total casualties by census block are shown in Figure 17. This map shows how the distribution of casualties at the census block level is redistributed, allowing a detailed and focalized view on where the higher the casualties counts are.

In the map, in Figure 17, some blocks incurred much higher numbers of casualties whereas others had very little or none as shown from the casualty counts. The census blocks that did not have any predicted casualties resulted to be either void of any buildings or there was little population, if any, expected within the buildings found in those blocks.

The results of casualties can also be viewed by land use. In this study area, only two land uses are expected to incur injuries under the UDSCE method. The vast majority of casualties were found in commercial buildings with a handful of casualties attributed

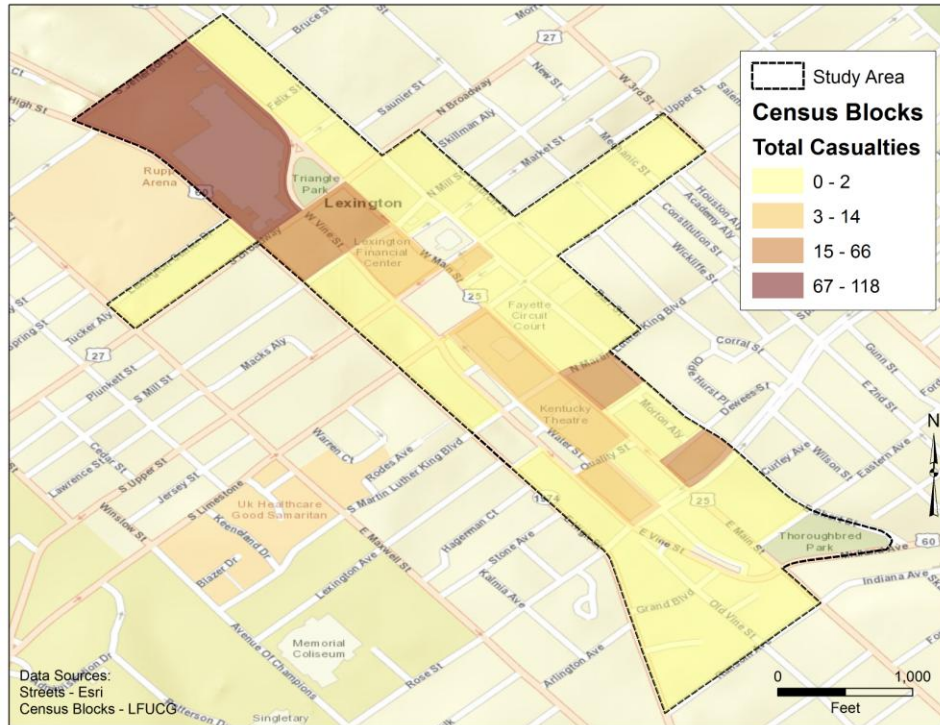


Figure 17 Estimation of Casualties by Census Block

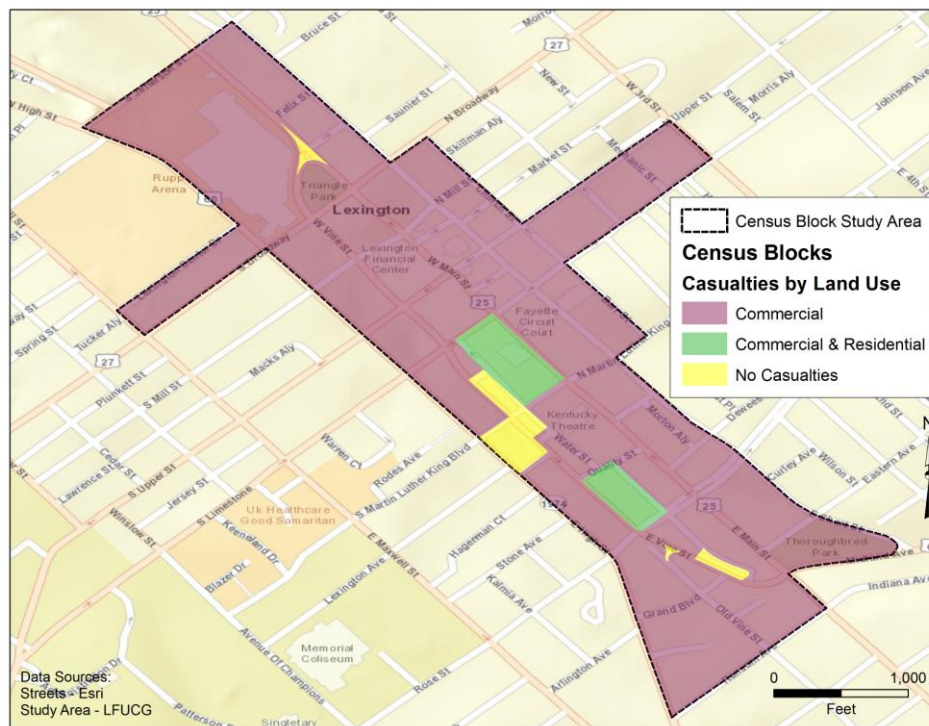


Figure 18 Census Block Casualties By Land Use. Casualties in Commercial land use estimated at 357, for Commercial & Residential at 14

to residential. The results of the casualties by land use are shown in Figure 18. The results from the UDSCE method at census block level are very promising and give a better understanding of the casualties distribution which could be extremely helpful to direct emergency responders in the areas where high casualty counts are present.

4.4 UDSCE Method at Parcel Level Results

A thematic map of the natural breaks classification of estimated casualties by parcel is shown in Figure 18. When viewing this map it is easily noticeable that many individual parcels are omitted. This is because these parcels were ruled out based on their criteria that indicated that no persons would likely be occupying the structure located there during the daytime hours, or that there is simply no structure on the parcel.

The casualties map at parcel level, in Figure 19, enable to outline in more detail the areas in which higher rate of casualties could occur, thus providing a better understanding of access scenarios to specific buildings for emergency responders.

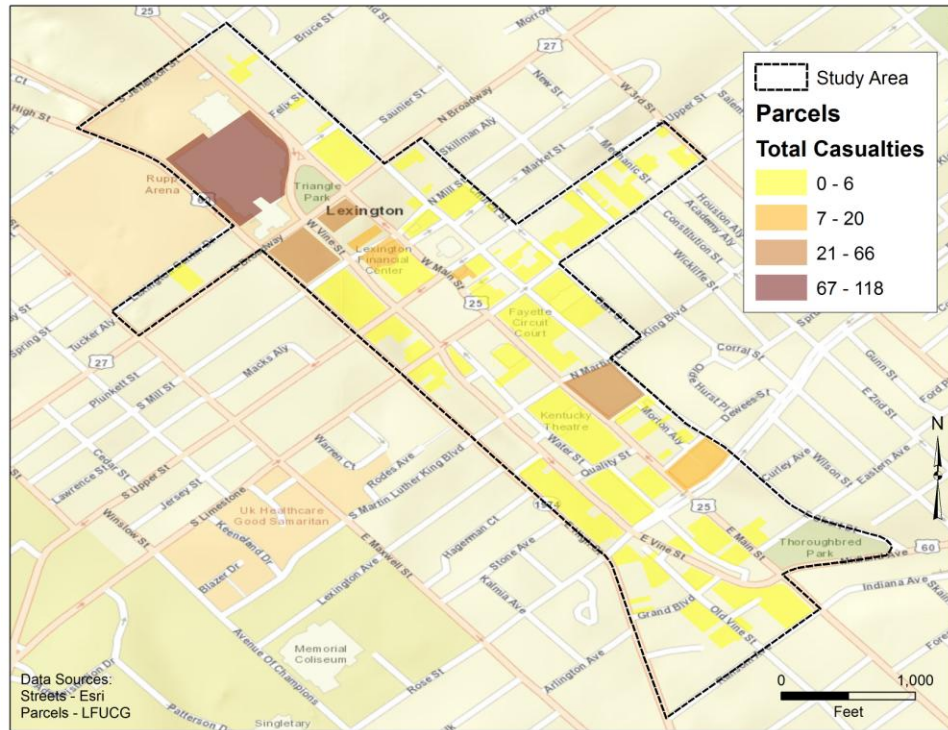


Figure 19 Estimation of Casualties by Parcel

CHAPTER 5: CONCLUSIONS AND FUTURE WORK

Chapter 5 summarizes the conclusions and insights on possible future steps that could be undertaken for the use and improvement of the new UDSCE method.

5.1 Conclusions

The HAZUS-MH application model earthquake casualties at the census tract level, hence the UDSCE method was designed to identify potential casualties at a higher resolution level in urbanized areas. The UDSCE method was validated with results from three HAZUS-MH models, at three different magnitude scenarios, for the census tract containing the CBD of Lexington, Kentucky. Casualties at higher resolution, in the urbanized area, were then calculated using the UDSCE method at a census block level.

The validation process of the UDSCE method went well overall. By comparing this method with three earthquake scenario models generated from HAZUS-MH, an indication was given of an approximate earthquake strength that the UDSCE method best models. The UDSCE method predicted 371 total casualties, putting it closer in line with the “Strong” 6.2 magnitude HAZUS-MH scenario at 289 casualties. In general the UDSCE method results overestimated casualties for Severity 1 and Severity 2 in a “Strong” earthquake case scenario while the Severity 3 and Severity 4 levels are underestimated, as evidenced by the Percent Difference Error analysis results in Table 17. The change in study area from the HAZUS-MH models to the UDSCE method was not a factor as the vast majority of casualties came from commercial buildings and 92.5 percent

of the commercial space within the HAZUS-MH census tract was located inside the block group study area utilized by the UDSCE method. This was a good indicator that the UDSCE method would be a competent alternative for earthquake casualty modeling to HAZUS-MH.

Once the UDSCE method was validated, the next step was to group the casualty count by census blocks for the high resolution analysis. This was done with the UDSCE method analysis at census block and individual parcels level. The resulting maps, shown in Figure 16, 17, and 18 (Section 4.3 and 4.4), outline how widely the injuries can vary within the study area. Only a handful of census blocks and parcels contained the majority of the total casualties, whereas many other blocks and parcels have shown very little or no casualties. Casualties by land use were also analyzed and clearly outlined that high casualties occurred in Commercial and Commercial & Residential land use categories, while only nine people were hurt that were not in a commercial building.

5.2 Future Work

The results in this study have shown the capability to outline where injuries could occur within the urbanized area at the block and parcels level, thus facilitating emergency response in the case of a powerful earthquake taking place during the daytime hours. However, improvements are possible and considerations for future work are discussed in the following sections in regard to data use, flexibility of the UDSCE method, areal constraints, population estimations and factors affecting the estimates.

5.2.1 Data Availability

The data used to develop the UDSCE method was derived from local sources. These sources included the PVA spreadsheet data, local government parcel shapefiles and LiDAR developed by a private business. The three primary parameters that made up the new UDSCE method were easily available and provided the necessary detail that for a solid model foundation, though improvements could be made especially when considering building parameters.

The PVA data provided general building material attributes but were not nearly as detailed as the building types that HAZUS-MH utilized. Better detail of construction of the buildings, such as knowing whether structures are reinforced with stronger materials on the inside, could enhance the scoring method and deliver better results.

Additional parameters should also be considered for future studies with the UDSCE method. One parameter in particular that would add value is the soil makeup of the study area. Soil type plays a part in determining the vulnerability of structures and can vary even in an urbanized area (Ploeger, Atkinson and Samson 2010).

5.2.2 Flexibility of UDSCE Method

The UDSCE method is suited for a specific type of study area (urban with a large commercial presence) and a specific time of day (in the middle of a day). This method would not be helpful for a study area made up of mostly residential areas. Hopefully, any future work done with this method would yield information that would help develop this methodology to assess vulnerability and casualties in places like residential areas.

The UDSCE method was also developed in a way so that it can easily be compared to the HAZUS-MH application, in accordance with earthquake hazard standards, for verification. The UDSCE method did not take into consideration the input that HAZUS-MH requires for its scenario such as epicenter coordinates, magnitude and depth, therefore the only way to verify the findings is to conduct multiple HAZUS-MH scenarios with different magnitudes and see how which one best resembled the UDSCE results. Potentially the same earthquake input scenarios could be implemented in the UDSCE method, however, more work must be done in this direction to allow users this advanced flexibility.

5.2.3 Study Area Constraints

The CBD of Lexington, Kentucky was selected for the trial run of the UDSCE method. This study area fit entirely within one census tract, which meant that there was only one census tract to compare between the HAZUS-MH and the UDSCE results for validation purposes, however, this could be a limitation in the validation process. Selecting an urbanized area containing multiple census tracts would lead to multiple comparison and increasing data would allow to refine indicators of the accuracy of the UDSCE method depending on the complexity of the urban scenarios. Future development of this method should consider analyzing data derived from multiple census tracts.

5.2.4 Population Estimations

Casualty estimations generated by the UDSCE method relied on a formula that estimated what the population would be within all structures located in the selected study

area. Square footage and land use were the two factors that were used in this study. Much more could be done to improve the accuracy of the population counts. For example, occupancy rates of office buildings and apartment complexes would be good information to know to improve upon the population estimation. Also, better knowledge of commuting populations would help with the development of a better population estimation formula.

5.2.5 Time Factors Affecting Estimates

Changes to the UDSCE method could help accurately predict casualties at other times of the day. A nighttime scenario would shift the focus to residential areas for assessing building vulnerability and calculating population for locating casualties. Depending on the study area, building height may be less relevant and LiDAR data may not be as useful for this purpose. However, LiDAR could be utilized for population estimations, as explained with examples in Section 1.2.3 in this study. These developments would open up the possibility to improving upon the HAZUS-MH method of estimating earthquake casualties of census tracts of residential areas.

REFERENCES

- Aydöner, C. and D. Maktav. April 2009. The role of the integration of remote sensing and GIS in land use/land cover analysis after an earthquake. *International Journal of Remote Sensing* 30(7): 1697-1717.
- Barazzetti, L., M. A. Brovelli and L. Valentini. 2010. LiDAR digital building models for true orthophoto generation. *Applied Geomatics*, 2(4): 187-196.
- Campbell, J. B. and R. H. Wynne 2011. *Introduction to Remote Sensing, Fifth Edition*. New York: The Guilford Press.
- Central United States Earthquake Consortium (CUSEC). 2013. Central U.S. Earthquake Consortium – CUSEC. <http://www.cusec.org/> (last accessed 29 September 2013)
- Dell'Acqua, F. and P. Gamba. October 2012. Remote sensing and earthquake damage assessment: experiences, limits, and perspectives. *Proceedings of the IEEE* 100 (10): 2876-2890.
- Dong, P., S. Ramesh, and A. Nepali. 10 November 2010. Evaluation of small-area population estimation using LiDAR, Landsat TM and parcel data. *International Journal of Remote Sensing*, 31(21): 5571-5586.
- Esri. October 2008. Geographic information systems providing the platform for comprehensive emergency management. <http://www.esri.com/industries/public-safety/~media/Files/Pdfs/library/whitepapers/pdfs/gis-platform-emergency-management.pdf> (last accessed 4 February 2014).
- Federal Emergency Management Agency (FEMA). 2014. Hazus. <http://www.fema.gov/hazus> (last accessed 4 February 2014).
- Geiß, C. and H. Taubenböck. August 2013. Remote sensing contributing to assess earthquake risk: from a literature review towards a roadmap. *Natural Hazards* 68(1): 7-48.
- Gillespie, T. W., J. Chu, E. Frankenburg, and D. Thomas. 2007. Assessment and prediction of natural hazards from satellite imagery. *Progress in Physical Geography* 31(5): 459-470.
- Güzey, Ö, E. Aksoy, A. C. Gel, Ö. Anil, N. Gültekin and S. O. Akbas. 2013. An interdisciplinary approach for earthquake vulnerability assessment in urban areas: A case study of Central District, Yalova. *Regional Studies Association, Annual European Conference*, University of Tampere, Tampere, Finland.

- Hashemi, M. and A. A. Alisheikh. 2011. A GIS-based earthquake damage assessment and settlement methodology. *Soil Dynamics and Earthquake Engineering*, 31: 1607-1617.
- HAZUS-MH. 2012. Version 2.1. Federal Emergency Management Agency. Washington, D.C., United States of America.
- Kentucky Geological Survey (KGS). 2013. <http://www.uky.edu/KGS/> (last accessed 10 November 2013).
- Kirscher, C. A., R. V. Whitman and W. T. Holmes. May 2006. HAZUS Earthquake Loss Estimation Methods. *Natural Hazards Review* 7: 45-59.
- Lexington/Fayette Urban County Government (LFUCG). 2013. Geographic Information Systems. <http://www.lexingtonky.gov/index.aspx?page=416> (last accessed 29 September 2013).
- Lexington-Fayette Property Valuation Administrator (PVA) Office. 2013. <http://fayette-pva.com> (last accessed 15 March 2014)
- Liu, J. G., P. J. Mason, E. Yu, M. C. Wu, C. Tang, R. Huang, and H. Liu. February 2012. GIS modeling of earthquake damage zones using satellite remote sensing and DEM data. *Geomorphology* 139-140: 518-535.
- Mauk, F. J., D. Christensen, and S. Henry. February 1982. The Sharpsburg, Kentucky earthquake 27 July 1980: main shock parameters and isoseismal maps. *Bulletin of the Seismological Society of America* 72(1): 221-236.
- Miller, N. 2012. Estimating Office Space per Worker. University of San Diego. <http://www.sandiego.edu/pipeline/documents/EstimatingOfficeSpaceRequirementsMay12012.pdf> (last accessed 13 November 2013).
- Moffatt, S. F. and T. J. Cova. 2010. Parcel-scale Earthquake Loss Estimation with HAZUS: A Case Study in Salt Lake County, Utah. *Cartography and Geographic Information Science* 37(1): 17-29.
- National Earthquake Hazards Reduction Program (NEHRP). 2014. <http://www.nehrp.gov/> (last accessed 4 February 2014). Neighbors, C. J., E. S. Cochran, Y. Caras and G. R. Noriega. 2013. Sensitivity Analysis of FEMA HAZUS Earthquake Model: Case Study from King County, Washington. *Natural Hazards Review* 14(2): 134-146.
- Ploeger, S. K., G. M. Atkinson and C. Samson. 2010. Applying the HAZUS-MH software tool to assess seismic risk in downtown Ottawa, Canada. *Natural Hazards* 53: 1-20.

- Qiu, F., H. Sridharan, and Y. Chun. July 2010. Spatial autoregressive model for population estimation at the census block level using LIDAR-derived building volume information. *Cartography and Geographic Information Science*, 37(3): 239-257.
- Remo, J. W. F. and N. Pinter. 2012. HAZUS-MH earthquake modeling in the central USA. *Natural Hazards* 62: 1055-1081.
- Sahar, L., S. Muthukumar, and S. P. French. September 2010. Using aerial imagery and GIS in automated building footprint extraction and shape recognition for earthquake risk assessment of urban inventories. *Transactions on Geoscience and Remote Sensing* 48 (9): 3511-3520.
- Sampath, A. and J. Shan. 2007. Building boundary tracing and regularization from airborne LIDAR point clouds. *Photogrammetry Engineering Remote Sensing*, 73(7): 805–812.
- Show Me Net. 2014. New Madrid Seismic Zone.
<http://www.showme.net/~fkeller/quake/comments.htm> (last accessed 16 June 2014)
- Silván-Cárdenas, J. L., L. Wang, P. Rogerson, C. Wu, T. Feng, and B. D. Kamphaus. 2010. Assessing fine-spatial-resolution remote sensing for small-area population estimation. *International Journal of Remote Sensing*, 31(21): 5605-5634.
- Street, R. August 1982. Ground motion values obtained from the 27 July 1980 Sharpsburg, Kentucky earthquake. *Bulletin of the Seismological Society of America* 72(4): 1295-1307.
- The Business Journals. 18 April 2008. Earthquakes Shake Louisville Area.
<http://www.bizjournals.com/louisville/stories/2008/04/14/daily36.html> (last accessed 5 March 2014).
- United States Census Bureau. 2013. <http://www.census.gov> (last accessed 20 December 2013).
- United States Geological Survey (USGS). 2014. Building Safer Structures.
<http://earthquake.usgs.gov/learn/publications/saferstructures> (last accessed 2 February 2014).
- University of California, Davis. 2014.
<http://www.physics.ucdavis.edu/Classes/Physics9Lab/Phy9BLab/9ASupplements.pdf> (last accessed 6 June 2014).
- UPSeis. 2014. <http://www.geo.mtu.edu/UPSeis/magnitude.html> (last accessed 4 June 2014).

Vanarsdale, R. November 1986. Quaternary displacement on faults within the Kentucky River fault system of east-central Kentucky. *Geological Society of America Bulletin* 97: 1382-1392.

APPENDIX A: Indoor Casualty Rates by Model Building Type for Slight Structural Damage

#	Building Type (Appendix F)	Severity 1 (%)	Severity 2 (%)	Severity 3 (%)	Severity 4 (%)
1	W1	0.05	0	0	0
2	W2	0.05	0	0	0
3	S1L	0.05	0	0	0
4	S1M	0.05	0	0	0
5	S1H	0.05	0	0	0
6	S2L	0.05	0	0	0
7	S2M	0.05	0	0	0
8	S2H	0.05	0	0	0
9	S3	0.05	0	0	0
10	S4L	0.05	0	0	0
11	S4M	0.05	0	0	0
12	S4H	0.05	0	0	0
13	S5L	0.05	0	0	0
14	S5M	0.05	0	0	0
15	S5H	0.05	0	0	0
16	C1L	0.05	0	0	0
17	C1M	0.05	0	0	0
18	C1H	0.05	0	0	0
19	C2L	0.05	0	0	0
20	C2M	0.05	0	0	0
21	C2H	0.05	0	0	0
22	C3L	0.05	0	0	0
23	C3M	0.05	0	0	0
24	C3H	0.05	0	0	0
25	PC1	0.05	0	0	0
26	PC2L	0.05	0	0	0
27	PC2M	0.05	0	0	0
28	PC2H	0.05	0	0	0
29	RM1L	0.05	0	0	0
30	RM1M	0.05	0	0	0
31	RM2L	0.05	0	0	0
32	RM2M	0.05	0	0	0
33	RM2H	0.05	0	0	0
34	URML	0.05	0	0	0
35	URMM	0.05	0	0	0
36	MH	0.05	0	0	0

Source: HAZUS-MH (2013)

APPENDIX B: Indoor Casualty Rates by Model Building Type for Moderate Structural Damage

#	Building Type (Appendix F)	Severity 1 (%)	Severity 2 (%)	Severity 3 (%)	Severity 4 (%)
1	W1	0.25	0.030	0	0
2	W2	0.20	0.025	0	0
3	S1L	0.20	0.025	0	0
4	S1M	0.20	0.025	0	0
5	S1H	0.20	0.025	0	0
6	S2L	0.20	0.025	0	0
7	S2M	0.20	0.025	0	0
8	S2H	0.20	0.025	0	0
9	S3	0.20	0.025	0	0
10	S4L	0.25	0.030	0	0
11	S4M	0.25	0.030	0	0
12	S4H	0.25	0.030	0	0
13	S5L	0.20	0.025	0	0
14	S5M	0.20	0.025	0	0
15	S5H	0.20	0.025	0	0
16	C1L	0.25	0.030	0	0
17	C1M	0.25	0.030	0	0
18	C1H	0.25	0.030	0	0
19	C2L	0.25	0.030	0	0
20	C2M	0.25	0.030	0	0
21	C2H	0.25	0.030	0	0
22	C3L	0.20	0.025	0	0
23	C3M	0.20	0.025	0	0
24	C3H	0.20	0.025	0	0
25	PC1	0.25	0.030	0	0
26	PC2L	0.25	0.030	0	0
27	PC2M	0.25	0.030	0	0
28	PC2H	0.25	0.030	0	0
29	RM1L	0.20	0.025	0	0
30	RM1M	0.20	0.025	0	0
31	RM2L	0.20	0.025	0	0
32	RM2M	0.20	0.025	0	0
33	RM2H	0.20	0.025	0	0
34	URML	0.35	0.400	0.001	0.001
35	URMM	0.35	0.400	0.001	0.001
36	MH	0.25	0.030	0	0

Source: HAZUS-MH (2013)

APPENDIX C: Indoor Casualty Rates by Model Building Type for Extensive Structural Damage

#	Building Type (Appendix F)	Severity 1 (%)	Severity 2 (%)	Severity 3 (%)	Severity 4 (%)
1	W1	1	.1	0.001	0.001
2	W2	1	.1	0.001	0.001
3	S1L	1	.1	0.001	0.001
4	S1M	1	.1	0.001	0.001
5	S1H	1	.1	0.001	0.001
6	S2L	1	.1	0.001	0.001
7	S2M	1	.1	0.001	0.001
8	S2H	1	.1	0.001	0.001
9	S3	1	.1	0.001	0.001
10	S4L	1	.1	0.001	0.001
11	S4M	1	.1	0.001	0.001
12	S4H	1	.1	0.001	0.001
13	S5L	1	.1	0.001	0.001
14	S5M	1	.1	0.001	0.001
15	S5H	1	.1	0.001	0.001
16	C1L	1	.1	0.001	0.001
17	C1M	1	.1	0.001	0.001
18	C1H	1	.1	0.001	0.001
19	C2L	1	.1	0.001	0.001
20	C2M	1	.1	0.001	0.001
21	C2H	1	.1	0.001	0.001
22	C3L	1	.1	0.001	0.001
23	C3M	1	.1	0.001	0.001
24	C3H	1	.1	0.001	0.001
25	PC1	1	.1	0.001	0.001
26	PC2L	1	.1	0.001	0.001
27	PC2M	1	.1	0.001	0.001
28	PC2H	1	.1	0.001	0.001
29	RM1L	1	.1	0.001	0.001
30	RM1M	1	.1	0.001	0.001
31	RM2L	1	.1	0.001	0.001
32	RM2M	1	.1	0.001	0.001
33	RM2H	1	.1	0.001	0.001
34	URML	2	.2	0.002	0.002
35	URMM	2	.2	0.002	0.002
36	MH	1	.1	0.001	0.001

Source: HAZUS-MH (2013)

APPENDIX D: Indoor Casualty Rates by Model Building Type for Complete Structural Damage (No Collapse)

#	Building Type (Appendix F)	Severity 1 (%)	Severity 2 (%)	Severity 3 (%)	Severity 4 (%)
1	W1	5	1	0.01	0.01
2	W2	5	1	0.01	0.01
3	S1L	5	1	0.01	0.01
4	S1M	5	1	0.01	0.01
5	S1H	5	1	0.01	0.01
6	S2L	5	1	0.01	0.01
7	S2M	5	1	0.01	0.01
8	S2H	5	1	0.01	0.01
9	S3	5	1	0.01	0.01
10	S4L	5	1	0.01	0.01
11	S4M	5	1	0.01	0.01
12	S4H	5	1	0.01	0.01
13	S5L	5	1	0.01	0.01
14	S5M	5	1	0.01	0.01
15	S5H	5	1	0.01	0.01
16	C1L	5	1	0.01	0.01
17	C1M	5	1	0.01	0.01
18	C1H	5	1	0.01	0.01
19	C2L	5	1	0.01	0.01
20	C2M	5	1	0.01	0.01
21	C2H	5	1	0.01	0.01
22	C3L	5	1	0.01	0.01
23	C3M	5	1	0.01	0.01
24	C3H	5	1	0.01	0.01
25	PC1	5	1	0.01	0.01
26	PC2L	5	1	0.01	0.01
27	PC2M	5	1	0.01	0.01
28	PC2H	5	1	0.01	0.01
29	RM1L	5	1	0.01	0.01
30	RM1M	5	1	0.01	0.01
31	RM2L	5	1	0.01	0.01
32	RM2M	5	1	0.01	0.01
33	RM2H	5	1	0.01	0.01
34	URML	10	2	0.02	0.02
35	URMM	10	2	0.02	0.02
36	MH	5	1	0.01	0.01

Source: HAZUS-MH (2013)

APPENDIX E: Indoor Casualty Rates by Model Building Type for Complete Structural Damage (With Collapse)

#	Building Type (Appendix F)	Severity 1 (%)	Severity 2 (%)	Severity 3 (%)	Severity 4 (%)
1	W1	40	20	3	5
2	W2	40	20	5	10
3	S1L	40	20	5	10
4	S1M	40	20	5	10
5	S1H	40	20	5	10
6	S2L	40	20	5	10
7	S2M	40	20	5	10
8	S2H	40	20	5	10
9	S3	40	20	3	5
10	S4L	40	20	5	10
11	S4M	40	20	5	10
12	S4H	40	20	5	10
13	S5L	40	20	5	10
14	S5M	40	20	5	10
15	S5H	40	20	5	10
16	C1L	40	20	5	10
17	C1M	40	20	5	10
18	C1H	40	20	5	10
19	C2L	40	20	5	10
20	C2M	40	20	5	10
21	C2H	40	20	5	10
22	C3L	40	20	5	10
23	C3M	40	20	5	10
24	C3H	40	20	5	10
25	PC1	40	20	5	10
26	PC2L	40	20	5	10
27	PC2M	40	20	5	10
28	PC2H	40	20	5	10
29	RM1L	40	20	5	10
30	RM1M	40	20	5	10
31	RM2L	40	20	5	10
32	RM2M	40	20	5	10
33	RM2H	40	20	5	10
34	URML	40	20	5	10
35	URMM	40	20	5	10
36	MH	40	20	3	5

Source: HAZUS-MH (2013)

APPENDIX F: Explanation of Building Types

#	Building Type	Description
1	W1	Wood Light Frame >5,000 sq. ft.
2	W2	Wood Commercial and Industrial <5,000 sq. ft.
3	S1L	Steel Moment Frame Low-Rise (1-3 stories)
4	S1M	Steel Moment Frame Mid-Rise (4-7 stories)
5	S1H	Steel Moment Frame High-Rise (8 + stories)
6	S2L	Steel Braced Frame Low-Rise (1-3 stories)
7	S2M	Steel Braced Frame Mid-Rise (4-7 stories)
8	S2H	Steel Braced Frame High-Rise (8 + stories)
9	S3	Steel Light Frame
10	S4L	Steel Frame with Cast-in-Place Concrete Shear Walls Low-Rise (1-3 stories)
11	S4M	Steel Frame with Cast-in-Place Concrete Shear Walls Mid-Rise (4-7 stories)
12	S4H	Steel Frame with Cast-in-Place Concrete Shear Walls High-Rise (8 + stories)
13	S5L	Steel Frame with Unreinforced Masonry Infill Walls Low-Rise (1-3 stories)
14	S5M	Steel Frame with Unreinforced Masonry Infill Walls Mid-Rise (4-7 stories)
15	S5H	Steel Frame with Unreinforced Masonry Infill Walls High-Rise (8 + stories)
16	C1L	Concrete Moment Frame Low-Rise (1-3 stories)
17	C1M	Concrete Moment Frame Mid-Rise (4-7 stories)
18	C1H	Concrete Moment Frame High-Rise (8 + stories)
19	C2L	Concrete Shear Wall Low-Rise (1-3 stories)
20	C2M	Concrete Shear Wall Mid-Rise (4-7 stories)
21	C2H	Concrete Shear Wall High-Rise (8 + stories)
22	C3L	Concrete Frame with Unreinforced Masonry Infill Walls Low-Rise (1-3 stories)
23	C3M	Concrete Frame with Unreinforced Masonry Infill Walls Mid-Rise (4-7 stories)
24	C3H	Concrete Frame with Unreinforced Masonry Infill Walls High-Rise (8 + stories)
25	PC1	Precast Concrete Tilt-up Walls
26	PC2L	Precast Concrete Frames with Concrete Shear Walls Low-Rise (1-3 stories)
27	PC2M	Precast Concrete Frames with Concrete Shear Walls Mid-Rise (4-7 stories)
28	PC2H	Precast Concrete Frames with Concrete Shear Walls High-Rise

		(8 + stories)
29	RM1L	Reinforced Masonry Bearing Walls with Wood or Metal Deck Diaphragms Low-Rise (1-3 stories)
30	RM1M	Reinforced Masonry Bearing Walls with Wood or Metal Deck Diaphragms Mid-Rise (4 + stories)
31	RM2L	Reinforced Masonry Bearing Walls with Precast Concrete Diaphragms Low-Rise (1-3 stories)
32	RM2M	Reinforced Masonry Bearing Walls with Precast Concrete Diaphragms Mid-Rise (4-7 stories)
33	RM2H	Reinforced Masonry Bearing Walls with Precast Concrete Diaphragms High-Rise (8 + stories)
34	URML	Unreinforced Masonry Bearing Walls Low-Rise (1-2 stories)
35	URMM	Unreinforced Masonry Bearing Walls Mid-Rise (3 + stories)
36	MH	Mobile Homes

Source: HAZUS-MH (2013)